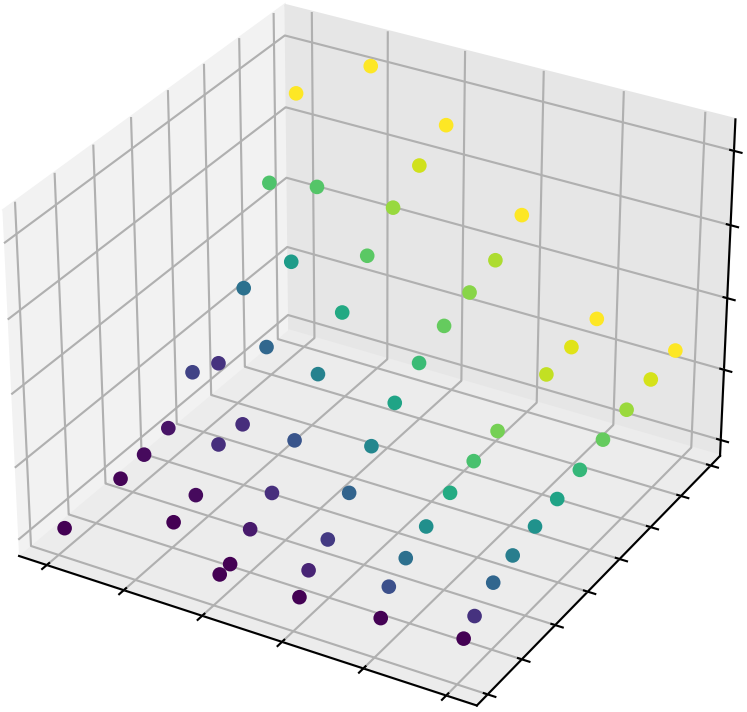

Creating an Algorithm for Hard Landing Detection using Aircraft Flight Data

Master's thesis in Applied Mechanics

FREDRIK ANGERVALL
JACOB GUNNARSSON

DEPARTMENT OF INDUSTRIAL AND MATERIALS SCIENCE

CHALMERS UNIVERSITY OF TECHNOLOGY
Gothenburg, Sweden 2023
www.chalmers.se

Master's thesis 2023

Creating an Algorithm for Hard Landing Detection using Aircraft Flight Data

FREDRIK ANGERVALL
JACOB GUNNARSSON

CHALMERS
UNIVERSITY OF TECHNOLOGY

Department of Industrial and Materials Science
Division of Material and Computational Mechanics
Chalmers University of Technology
Gothenburg, Sweden 2023

Creating an Algorithm for Hard Landing Detection using Aircraft Flight Data
FREDRIK ANGERVALL
JACOB GUNNARSSON

Supervisor: Fatih Cetin, Heart Aerospace AB
Supervisor: Alan Scott, Heart Aerospace AB
Examiner: Magnus Ekh, Department of Industrial and Materials Science

Master's Thesis 2023
Department of Industrial and Materials Science
Division of Material and Computational Mechanics
Chalmers University of Technology
SE-412 96 Gothenburg
Telephone +46 31 772 1000

Cover: Scattered plot of a part of the database.

Typeset in LaTeX

Creating an Algorithm for Hard Landing Detection using Aircraft Flight Data
FREDRIK ANGERVALL
JACOB GUNNARSSON
Department of Industrial and Materials Science
Chalmers University of Technology

Abstract

Aircraft hard landings can cause damage to a landing gear or aircraft frame which in turn can cause a critical failure. As such, methods to detect hard landings have been created in different ways, for example, based on a pilot's judgment or adding various sensors to a landing gear.

The aim of the thesis is to identify existing hard landing detection methods and compare them in order to find a suitable concept to further evaluate in regards to application in a commercial aircraft. The literature review of current hard landing detection methods and interviews with aerospace engineers showed that using flight data parameters was a promising concept.

A load predicting algorithm was created and tested in order to evaluate the concept. To make the algorithm, a CAD model of an arbitrary main landing gear (MLG) was first built for implementation in a multi-body dynamic model. This was then used to create a database of landing gear responses for different drop test simulations. Through sweeps over relevant parameters, longitudinal and normal tire forces were obtained for a spread of drop tests.

The database was then used in the algorithm, based on an interpolation scheme, to give tire longitudinal and normal forces as an output at three critical instances. The outputs could in the future be used to decide whether a hard landing has occurred or not by comparing them to limits. It became evident that a good database is necessary for the algorithm to provide proper force estimations.

The algorithm was accurate for an assumed runway friction. However, for a lower friction, the estimated forces were inaccurate. An alternative method using the angular velocity of the wheel to estimate the longitudinal force independent of friction was tested. While simplifications were made, it was shown that the method gave better estimations for low friction.

Using aircraft flight parameters for detecting hard landings was proved to be a concept with potential. For implementation in commercial use however, several points were identified as requirements for it to be a reliable method with high fidelity and functionality.

Keywords: Structural Health Monitoring, Hard Landing Detection, Drop Test Simulation, Aircraft Landing Gear

Acknowledgements

We would like to thank our supervisors, Fatih Cetin and Alan Scott at Heart Aerospace, for the extensive help and discussions during the thesis. We would also like to thank our examiner Magnus Ekh, professor at the Division of Material and Computational Mechanics, for his valuable input. Further, we express our gratitude to Heart Aerospace and all employees who showed an interest in the thesis topic.

Fredrik Angervall & Jacob Gunnarsson, Gothenburg, June 2023

List of Acronyms

Below is the list of acronyms that have been used throughout this thesis listed in alphabetical order:

AoG	Aircraft on Ground
CoG	Center of Gravity
CRES	Corrosion resistant steel
FDR	Flight Data Recorder
IMU	Inertial Measuring Unit
MLG	Main Landing Gear
MTOM	Maximum Take-Off Mass
NLG	Nose Landing Gear
SHM	Structural Health Monitoring
S/A	Shock Absorber
VAT	Vertical Axis Travel

Contents

List of Figures

List of Tables

1
Introduction

1.1 Background

In the aviation industry, many parts in aircraft design are made to be damage tolerant where inspections are performed regularly to monitor the health and expected life until a critical service is issued. Damage tolerant design is the concept of defining critical crack lengths and inspection intervals, making sure that cracks are found during inspection before they become critical. The inspections are performed through non-destructive testing (NDT), which can in some cases be cumbersome or difficult in itself.

However, damage tolerant design is not of consideration in this thesis since it is not used in landing gears due to impracticality. Landing gears are highly loaded yet need to be light and possible to fold away, thus use of high strength materials and single load path design is necessary. This will typically lead to small critical crack lengths and short inspection intervals with burdensome techniques. Instead, a safe life design is utilized, meaning that no crack initiation, or propagation for that matter, is allowed and the landing gear is replaced when this life is reached as mentioned in SAE International AIR6813 [1] and Infosys publication [2]. The design is made for the worst landing loads expected in service, see SAE International AIR5938A [3]. Landing loads can in extreme conditions such as a crash landing exceed the expected limits used for design, where permanent damage would be expected. Overload detection of some sort is often implemented to alert for hard landings or other abnormal loads which may lead to damage to any part of the landing gears.

Different types of damage that can occur during a hard landing are cracks, bent parts and fluid leakage [3]. These can usually be seen during a visual inspection. Further, overloads from a hard landing can induce residual stresses which are difficult to detect. Residual stresses can cause premature failure due to fatigue or stress corrosion cracking [1] of landing gear components.

As a current standard, the detection of hard landings or other high load cases on landing gears is not always effectively implemented. There are many implementations of monitoring systems that alert for certain overloads. They can be based on aircraft sink rate, aircraft g-sensor readings, load sensors or strain gauges amongst other methods. These are often used in combination with a pilot stating that a hard or deviating landing has occurred to warrant an Aircraft on Ground (AoG) state

and an inspection for landing gear damage performed.

In some aircraft the data may actually lead to the waiving of some or all inspections warranted after a hard landing declaration if the measured loads are below a certain threshold, see SAE International AIR6168A [4]. In fact, in many cases the subjective pilot judgement is on the safe side and leads to unnecessary investigations, thus grounding a capable aircraft as well as requiring staff to perform a service. These aspects lead to an economic burden as discussed in Bradley [5].

There are also implementations of overload detection which are more complex, for example layers of overloads, see AIR5938A [3]. It deploys levels of inspections, where for extreme loads a grounding is issued directly and the load data is sent to the landing gear manufacturer in order to evaluate the landing in combination with an inspection to assess the damage. The second level for high but not extreme loads is sending the data to the landing gear manufacturer and allowing the aircraft to continue service for a limited time, or until the landing gear manufacturer has been able to process the data to conclude if damage may have occurred and an inspection should be performed.

Clearly, in order to avoid an unnecessary AoG state which leads to both loss of revenue when an aircraft is not in service and expensive and time consuming services to be performed, there is a need to implement some type of Structural Health Monitoring (SHM) of landing gears in aircraft. Implementing an SHM method which can detect high load cases reliably such that AoG declarations could be reduced and an aircraft may be utilized with fewer interruptions is not a new concept. The methods mentioned in this chapter are some of many alternatives, but several concepts chosen for consideration are described in greater detail in the next chapter of the report.

1.2 Aim

The aim of the project is to identify and evaluate the latest SHM approaches applicable to an aircraft landing gear with the main objective of monitoring hard landings. Further, options which can be evaluated for use on an actual aircraft should be proposed. From the identified methods, one will be selected based on identified criteria and further investigated to conclude complexity, usability and reliability amongst other aspects of the method and if it is viable for use in aircraft.

The investigation entails creating an algorithm that should be able to detect a hard landing overload and evaluating the reliability of detection. For investigating the complexity and usability, the possibilities of implementing the concept in commercial aircraft will be considered.

1.3 Limitations

There will not be a prototype or test performed on existing components in order to evaluate the functionality of the multi-body dynamic model or algorithm for overload detection. Increasing fatigue life may or may not be included in the consideration and evaluation of the selected method. A dummy landing gear model in combination with arbitrary aircraft mass will be used for dynamic simulations of hard landing events. The investigation will be performed based on a single landing gear, thus a full aircraft model is not considered.

1.4 Investigated issues

- What current SHM techniques exist for landing gears and what are the pros and cons? This includes aspects such as reliability, installation complexity, service and maintenance required, implementation complexity, data management and cost efficiency.

- From the identified concepts, formulate requirements for use in commercial aircraft and evaluate based on identified criteria. Choose a specific concept to investigate further.

- How is the landing gear behaviour determined in different landing scenarios by multi-body dynamic simulations? Perform simulations for nominal and hard landing cases in order to obtain the landing gear loads for these.

- Identify what type of algorithm that is needed for the chosen concept, in order to have the measured data from the concept as an input and to provide an overload statement as an output.

- Create an algorithm that, based on a specific concept, should be able to detect overloads. Evaluate the algorithm based on complexity, usability and reliability in commercial aircraft operation.

- Can the specific concept be used in order to monitor fatigue life of a landing gear? If so, is it necessary to measure all loads, accelerations or strains for example, and perform fatigue life estimation of the landing gear in order to prolong the safe life design? Could the fatigue life estimation be used to indicate that the safe life design is an overestimation based on what loads a specific aircraft has been subjected to during use?

1.5 Social, ethical and ecological aspects

The lowered cost in servicing because of the SHM may pave way for safer and better aviation. Hence, aircraft may continue to service longer with less environmental effects while still enabling a connected world.

If the SHM technique is implemented but incorrect data is gathered, the landing gear could suddenly fail.

If a way of measuring fatigue is implemented it can be used to prolong the life of the landing gear which will lower the cost and the environmental effect of the landing gear. It could also mean that a lower life than expected is detected which would mean that an accident can be prevented.

2
Concept evaluation and selection

This chapter covers several existing SHM techniques for aircraft landing gears. From the concepts, pros and cons have been identified, see table 2.1. An elimination of the listed concepts has been performed based on formulated requirements. Further, an evaluation has been conducted through a scored weighted decision matrix based on identified criteria relevant to the thesis contents and aspects in the aircraft industry. The listed concepts are grouped in order to simplify the elimination process. However, they are scored individually in the weighted decision matrix. More concepts can be found in AIR6168A [4], from which the listed concepts of interest are also retrieved.

2.1 Existing SHM techniques

Descriptions of some interesting existing SHM techniques, retrieved from AIR6168A [4] are presented below. The concepts are divided into groups used in the following concept elimination process.

2.1.1 Mechanical measurements

Purely mechanical methods of measuring overloads could be argued to be the least complex available. These concepts are potential solutions if only one load is required, and can easily give a visual indication if a design load has been exceeded without the need for processing data. However, the general problem and main drawback is that multidimensional loads, which is the majority of the critical loads, cannot be completely captured and the information gathered by mechanical measurements is for these cases generally low. Further, proper calibration and trigger levels are usually difficult to obtain. Some mechanical methods are still listed, since the simple systems could be useful, but they also provide a good understanding of why more advanced systems often are implemented.

2.1.1.1 Permanent deformation mechanisms

There are examples of shock absorbers (S/A) where a hard indenter has been mounted opposite to a softer material that would be marked by the indenter if the shock absorber compression exceeds a nominal stroke. This could be used to detect hard landings with higher than nominal decent rates or heavy landing weights since the shock absorber would be compressed further than nominally.

The benefits of this concept are the very easy implementation and the ease of detection when performing an inspection of the landing gear. The drawbacks, other than the fact that a small number of critical loads can be detected, are that the softer plate would need to be replaced after a hard landing and that an inspection for it would need to take place. Further, the magnitude of the overload is not possible to determine from an indentation and the general problems of shock absorber servicing state (gas and fluid levels). This in combination with aspects such as potential gas and oil dissolution and friction heating the damper fluid are parameters that can affect the detection.

2.1.1.2 Structural 'fuses'

Introducing a structural element acting as a fuse in the landing gear is another way of performing mechanical measurements. The concept is based on the fact that the structural element fails noticeably when overloaded. An approach of this could be to have a part that fails but another part that takes over as the load carrying part that has sufficient load carrying capacity for the whole landing gear to not fail. A specific approach is the Safran Landing Systems approach, described in AIR6168A [4, Sec. 5.2], of a so called pin with a pin, where a thin shelled fuse pin fails when overloaded while a backup pin inside it carries enough load for maintaining structural integrity. For these applications, a dye or some other visual indication can be contained between the two pins such that a clear visual indication is given when an overload has occurred.

The primary benefits are the low complexity of implementation and the clear visual indication when inspecting. The drawbacks are similar to the permanent deformation mechanisms, meaning that a visual inspection is needed and that the structural member needs to be replaced. More drawbacks are the difficulty to calibrate when failure should occur and of course the low information given by one-dimensional load indications while most landing gear critical loads are multi-dimensional.

2.1.2 Dynamic measurements

Dynamic measurements such as accelerometers or potentiometers can generally provide better information than purely mechanical measurements. The reason is that the dynamic behavior can be monitored and loads can often be detected in more than one direction. Dynamic measurements exist with various complexities. General for most concepts is that a model is needed to interpret loads or strains from the dynamic measurements. This may become a problem depending on the concept. The models require approximations of some flight parameters such as aircraft Center of Gravity (CoG), ground friction or shock absorber servicing state. This means that some error in the estimated loads are inherent. Further, time stamping could pose an issue when introducing several sensors, such that the measured data may provide an incorrect state of an aircraft when combined. A few methods for consideration are described in this thesis, however, AIR6168A [4] includes more.

2.1.2.1 Using aircraft flight data recorder accelerometer

The main benefit of utilizing the already existing flight data instruments is that no extra system complexity is introduced. But there are several drawbacks to this simple dynamic method, mainly that the sampling rate of the accelerometers needed for landing peak load detection may be higher than what is needed for aircraft operation. The analysis to relate the aircraft accelerations to landing gear loads may thus be complicated. As such, the use of this method has in early applications been used to indicate a hard landing instead of providing information of the actual overloads. More advanced concepts exist and one is covered in section 2.1.2.3. There are potentials to use the data in combination with other methods, where the hard landing indication may be done by the flight data. Further problems with this concept are, as general with the dynamic measurements of detecting other than hard landings, for example, ground maneuvering loads.

2.1.2.2 Multi-dimensional peak accelerometer

More advanced dynamic measurements include a system developed by Safran Landing Gears described in AIR6168A [4, Sec. 5.1]. It detects hard landings based on accelerations in three dimensions in combination with pitch, yaw and roll rates gathered from several Inertial Measurement Units (IMUs) located on the landing gear structure. The data gathered is combined for a complete approximation of the loads. The data is compared to predetermined thresholds to detect if a hard landing has occurred.

This system is easy to retrofit to any aircraft, which also means that the implementation to a landing gear is not too complex. Further benefits of the concept itself are that the sensors used can be placed on the landing gear to capture the landing gear behavior without interference from the aircraft's structural dynamic properties and that the hard landing indication is performed without the necessity of an inspection. The main drawbacks of the concept are that the data gathered may not capture the true loading behavior and the introduction of more sensors. This leads to higher risk of sampling issues and more calibration. As for other dynamic measurements, the concept may not be able to capture other ground loads such as taxi and tow loads, and it may be difficult to detect take-off overloads.

2.1.2.3 Boeing patented method in use in recent aircraft

Boeing has patented a method of detecting hard landings which is in use on recent aircraft. The concept is primarily based on flight parameters such as sink rate, CoG vertical load factor, pitch, yaw, roll, gross weight and CoG position during landing. The data is sent to the maintenance crew if the pilot declares a hard landing has occurred. Calculated limits of the data provide thresholds for overload occurrence, and these limits can be used to waive some or all inspections when a pilot has declared a hard landing if the logged data is below certain thresholds.

Considering the number of flight parameters that are included in the logged data the

estimation of the landing loads should be good, and the pilot's judgment is the main indication where the data is used in conjunction. Pilot indication is in most cases on the safe side as discussed in Bradley [5] which makes the concept probable to detect hard or abnormal landings where the data can be used for confirmation. The drawbacks are primarily gathering knowledge of all flight parameters, mainly mass and CoG parameters which vary for each flight. Other parameters that can affect the loading without detection in the gathered data are for example shock absorber servicing state and tire pressures. Also, unsure runway conditions may occur during landing where a critical load may be experienced while not captured by the logged data. Hence, it may be reasoned that it is not safe to waive inspection steps based on that data.

2.1.3 Strain gauges

Strain gauges can be used to directly measure strain in a component of the landing gear and they also allows for measuring strain in multiple directions. Nowadays strain gauges are mostly used for testing since it has some drawbacks. But a few concepts have been patented, for example attaching strain gauges to critical components. Bradley [5] has a concept where strain gauges are placed on the wheel axle to measure the ground loads in all directions with recommendations of placement.

Even though strain can be measured directly and in multiple directions there are a few drawbacks. If adhesive bonding is used to attach the strain gauge it may degrade over time and thus has to be protected from the environment. Furthermore, data will have to be processed and the strain gauges will have to be calibrated from time to time. The strain gauges will also have to have an update frequency high enough to capture the peak loads, generating large amounts of data.

Other types of strain gauges could be used with other pros and cons. One example is the fiber bragg sensor where wavelengths in a fiber optic cable is used to measure strain. This type of sensor gives an absolute measurement of strain and temperature change and does not have to be recalibrated. However, additional sensors are required to measure temperature as mentioned in Bradley [5, p. 22] and thus is a disadvantage because of the increasing amount of sensors. Further, while the optical sensors have good reliability, other aspects of a system like this are prone to fail in harsh conditions, such as fibre optic cables which are sensitive to sharp bending radius and fatigue which apply for retractable landing gears. Other optical strain gauges also exist and can be possible to utilize as mentioned in AIR6168A [4] and Bradley [5]. But they are not considered for concept selection in this thesis due to their even higher complexity.

2.1.4 Coatings

Coatings can be used as an indication of overload by applying a brittle paint, lacquer, a film or foil on components of the landing gear. It will crack or give a color change

when subjected to significant strain. The strain levels for cracking or color change need to be designed for when specifying the coating properties. Of interest is that some coatings can crack in the direction of the maximum principal stress meaning that the strain direction may be noticed. For color changing coatings, micro-capsules of color forming or developing materials are broken such that colored patches appear where the pressure has been high enough to break the micro-capsules.

Coatings are simple and cheap methods and no data needs to be gathered or processed to detect high strains, provided the coating properties are designed such that the limits are correct. However, coatings are most commonly found in lab environments and have not been thoroughly investigated in environments outside labs. This makes it difficult to know if implementation on a landing gear in use would be a viable option. Further, some materials are not fitting for coating use, such as chrome, and fatigue properties of coatings are not known. Especially in the harsh environments seen by aircraft landing gears and the temperature differences they are exposed to.

2.1.5 Shock absorber monitoring

Using the shock absorber state to monitor loads can be done by measuring the fluid and gas pressure in the shock absorber. Difficulties with monitoring loads by the pressure level are that the friction within the damper needs to be considered and that both the fluid and gas pressure is required to obtain the true loading on the shock absorber. In order to monitor these pressures, a more complicated shock absorber design is typically needed by including valves, tubes and actuators which in turn reduce the reliability of the landing gear. Further concerns are that the monitoring of the pressures only provides information of the load in the direction of the shock absorber stroke and it is crucial to have a properly serviced shock absorber to retrieve proper load calculations. For unseparated shock absorbers, it is particularly difficult to measure the loads. This is because the gas is partly dissolved in the fluid, and for increasing pressure levels, more gas may be dissolved in the fluid as described by Henry's law [8, p.417].

A currently proposed system based on this method is a concept marketed by Crane as AirWeighs, see AIR6168A [4, Sec. 5.3.4]. The concept employs Nance's method where a certain volume of fluid is added to and removed from the damper whereby the shock absorber is displaced and thus minimizing friction and stiction properties. These are crucial aspects to consider for shock absorber monitoring to obtain proper measurements. This system allows for measuring shock absorber fluid levels and monitoring landing gear shock absorber health and may be used to detect overloads, implemented by Airbus.

Shock absorber monitoring allows for more data and monitoring than only overload detection events and can thus be useful to implement when more aspects are considered than the primary thesis objective of landing gear health monitoring and overload detection. Drawbacks are the need to well know the shock absorber service

state and that the shock absorber design is more complex, making it less reliable. Further, the concept is one of the more complex concepts.

2.1.6 Load cells

Load cells are most often based on strain gauges, however, pneumatic and hydraulic load cells are some other types. Load cells have the benefit over strain gauges in that the electrical measurement retrieved corresponds to increased loads and not strains. As such, load cells are force transducers, and in landing gear applications the most relevant type of load cell are encapsulated force transducers in a load path. There are load cell applications that use the landing gear as a transducer but it requires expensive and complex manufacturing of the landing gear, and will not be considered in concept evaluation.

Instead, the focus is on a system developed by Safran Landing Systems based on replacing conventional pins with load measuring pins in a landing gear. These load measuring pins use strain gauges, but since the pin encapsulates the strain gauges from the environment many of the drawbacks of strain gauge application may be avoided. The load measuring pins can be mounted in several locations on the landing gear, for example in the wheel axle or landing gear pintle pin to measure the reaction forces of the entire landing gear.

The pros with load cells are that the loads are measured directly and in multiple directions and if placed at certain spots the load throughout most of the structure can be measured. The cons are that it could be expensive to implement if not considered in the original development of the landing gear and a large amount of data will have to be processed when using load cells. Further, for strain based load cells there is a probability that recalibration may be necessary.

2.2 Compilation of concepts pros and cons

From the descriptions of the concepts listed above, identified pros and cons are gathered in a compiled list for a better overview in table 2.1 below. The list is used to compare the concept groups in the concept evaluation process.

Table 2.1: Concept groups, summarized pros and cons

Concepts	**Pros**	**Cons**
Mechanical devices	• Easy to implement • No need for processing data • Easy to detect at visual inspection	• Generally only measures in one direction • Provides a small amount of information • Can be difficult to calibrate • Often needs to be replaced in case of hard landing • May depend on the service state of the shock absorber
Dynamic measurements	• Make use of already installed devices in some cases • Continuous data • No need for visual inspection in order to detect hard landing • Possibility of getting a reliable indication of overload	• Not a direct measurement of loads in the gear • Additional sensors increase mass and complexity • Potential time stamping problems • Model must be made based on measurements • Errors of calculated loads because of assumptions of unknowns during modeling • Can be complex • Based on the assumption that the service state of the shock absorber is correct • Higher sampling rates to detect load peaks • Difficult to interpret ground loads from data

Strain gauges	• Strain is measured directly • Load can be measured in all directions • Continuous data	• Must be encapsulated • Adhesive degradation • Can be difficult and expensive to mount • Potential time stamping problems • Need to process the data • Need to have a high update frequency • Some strain gauges require recalibration
Coatings	• Simple • No need for processing data • Easy to detect during visual inspection • May detect in multiple directions	• Provides a small amount of information • Have to be replaced • Primarily used in lab environment • Low knowledge of reliability • Low knowledge of fatigue properties
Pressure in Shock Absorber	• Shock absorber health detected as well • Measure vertical load directly • Continuous data	• Required knowledge of the amount of oil and gas • Complex system and difficult to replace sensors • Can only measure load in one direction • Makes the shock absorber less reliable • Must account for friction and stiction in shock absorber

Load cells	• Load is measured directly • Load can be measured in all directions • Can be used as a part of the landing gear	• Can be difficult and expensive to mount • Potential time stamping problems • Needs to process the data • Higher sampling rates to detect load peaks • May require recalibration if strain gauge based

2.3 Evaluation of concepts

In order to support the choice of concept to use in the thesis, an elimination was performed followed by a scoring using a weighted decision matrix [6] based on identified criteria. A viable concept was chosen based on the score as well as interviews with aircraft engineers.

2.3.1 Concept requirements

In order to eliminate non-viable concepts before the evaluation, some requirements were identified based on the literature study and these are stated below.

Ability to measure load or strain in multiple directions. Failure due to a hard landing can occur in any direction and often due to a combination of loads. It is therefore necessary to measure load in vertical, lateral and longitudinal direction.

Ability to measure the magnitude of the load or strain. In order to get an understanding of how severe the damage of the parts of the landing gear or the attachments is, it is necessary to determine the magnitude of the load/strain.

No replacement of parts in the measurement system for a suspected overload. No part of the measurement system should need to be replaced after detecting a possible overload to keep the maintenance cost and time of the landing gear low.

Other possible requirements could be maximum cost, maximum mass, installation time, etc. However these are not considered as requirements for the thesis since no hard boundaries are considered (which may be the case in a true commercial process). Rather, these aspects are used for some of the identified criteria in order to compare remaining concepts in the concept evaluation stage.

Table 2.2: Elimination matrix

	Mechanical devices	Dynamic measurements	Strain gauges	Coatings	Pressure in shock absorber	Load cells
Measure in 3 directions	-	+	+	?	-	+
Can measure the magnitude of load or strain	-	+	+	-	+	+
No need to exchange parts in measurement system	-	+	+	-	+	+

2.3.2 Elimination of concepts

Based on the requirements a few concepts can be eliminated. In the elimination stage, the concepts were still grouped as in table 2.1 since the concepts within the groups are similar. The elimination matrix can be seen in table 2.2 where "-" means the requirement is not fulfilled, "+" means the requirement is fulfilled and "?" that more information is needed.

Since it can be difficult to measure load in multiple directions and to decide the magnitude of the loads when using mechanical devices, these were eliminated from further concept evaluation. Further for mechanical devices, parts usually need to be exchanged when a hard landing is indicated.

Another concept not fulfilling the requirements is coatings since the magnitude of the strain cannot be detected and the coating will have to be replaced with intervals. Furthermore, most coatings have only been used in lab environment which make them unreliable in the tough conditions to which landing gears are exposed. It may be noted that more information would be needed to determine the multi-dimension indication requirement. However, since the concept does not fulfill any of the other requirements this was not investigated.

Regarding shock absorber measuring, the concept is eliminated since it can only be used to measure load in the S/A stroke direction, not drag or lateral loads.

Concepts that fulfill all requirements were kept for evaluation using a weighted decision matrix. These were dynamic measurements, strain gauges and load cells. In order to generate a proper evaluation, a survey of interviews with aircraft engineers was performed.

2.3.3 Survey of potentials of concepts in aircraft

In order to perform an evaluation, further input than only from a literature study was required. As such, the concepts retained after performing the elimination were discussed with aircraft engineers in order to include experiences and opinions as well as to find out if these engineers had any input on hard landing detection in general.

From the interviews, it was found that the most important aspect to consider is the cost of the system which will influence the price for the customer. If a customer does not save money in the product life cycle by increasing the cost of the monitoring system, there will be no interest in the system all together. Another highlight from the interviews was that a customer does not want to add steps in the aircraft maintenance manual, since that would cause more work and more time spent on maintenance.

An example was given that, for a strain gauge or load cell to be calibrated, an aircraft would have to be put on jacks and the parts would have to be disassembled to apply a known load to set a new zero value for the measured resistance to correlate a correct strain. Further, it was pointed out that there are several benefits of using flight data, pilot reports and maintenance reports to start with and add additional sensors if needed to have a proper hard landing or overload detection system.

Another topic that was discussed is that in order to reduce the engineering workload to declare if a hard landing has occurred, the detection system should be automated so that an AoG statement does not have to be issued while investigating logged data. This would drastically reduce the financial burden for the manufacturer in terms of not having to investigate for each report, but also for the operator by better utilization of the aircraft.

The experience and opinion from the aircraft engineers were used in combination with what was found in the literature study to generate and weight criteria for evaluation in a weighted decision matrix.

2.3.4 Weighted decision matrix

A weighted decision matrix is a concept evaluation matrix that use weighted criteria to evaluate concepts. This was used to score concepts in correlation to each other. The generated matrix is presented in table 2.3 where an increasing score is better. The possible weights and scores were between 1 and 5. Note that aspects such as part design burden and design work hours were not considered, and the matrix thus evaluates the post-development aspects of each concept group.

The concepts were evaluated individually, contrary to the elimination step where they were grouped. Concepts are referred to as:

A - Using Flight Data
B - IMU on landing gear

C - Strain gauge
D - Load Cells

The identified criteria, including weights, were:

Reliability (Mechanical) is the mechanical reliability of the parts in the concepts. The weight is set to 5 since it is important to get the correct data and not have to maintain the system too often.

Data management simplicity is how much data which will have to be processed and how simple it is to evaluate the data. The weight is set to 2 since the remaining concepts do not differ drastically but data management has to be considered.

Cost efficiency is how expensive the system is including its parts, installation and maintenance but not the development cost. Here, a higher score means cheaper concept. The score was set to 5 due to the previously mentioned importance to keep the cost as low as possible.

System simplicity is a measurement of how many parts that are included in the system and how they are connected to each other. The weight is set to 2 because system complexity needs to be evaluated, however, should not be a deciding factor in itself but may rather be used as a finer evaluation for similarly scored concepts.

Ease of detection (overload) is how easy the overload is to detect from a pilot or maintenance personnel perspective. For example, if a visual inspection has to be performed or if it can be shown on the pilot's screen automatically. It is also a measurement of how useful the information that is gathered is to decide if a hard landing has occurred or not. The weight is set to 3 since it is important that the data can be easily interpreted but not as important as reliability, maintenance and cost.

Maintenance simplicity is how easy the system is to maintain and how often maintenance is needed. The weight is set to 5 since the objective of the project is to keep the maintenance of a landing gear low and it is therefore important to have a system which is easy to service and with low maintenance. From a selling point of view airlines rarely want to add additional features if the maintenance will increase.

Possibility of fatigue estimation is how well fatigue can be estimated with the concept. If fatigue estimation would not be possible to estimate, the score would be set to 0. The weight is set to 2 since it is not the main target of the system but it could be used and may be considered as a potential following investigation in the thesis.

Table 2.3: Weighted decision matrix

		Ideal		A		B		C		D	
Criteria	**W**	v	t	v	t	v	t	v	t	v	t
Reliability (mechanical)	5	5	25	5	25	4	20	2	10	3	15
Data management simp.	2	5	10	4	8	2	4	3	6	3	6
Cost efficiency	5	5	25	5	25	3	15	2	10	2	10
System simplicity	2	5	10	5	10	2	4	2	4	3	6
Ease of detection	3	5	15	3	9	4	12	5	15	5	15
Maintenance simplicity	5	5	25	5	25	4	20	2	10	2	10
Fatigue estimation	2	5	10	2	4	3	6	5	10	5	10
Total scoring		35	**120**	29	**106**	22	**81**	21	**65**	23	**72**

As can be seen in the weighted decision matrix, the mechanical reliability of using flight data is rated better than the other types since no extra system complexity is added and is deemed to be a robust system. Strain gauges and load cells are scored lower since the sensors and cables will be exposed to tough environmental conditions. There is also the aspect of cable fatigue due to repeated retraction and extension of the landing gears.

For data management simplicity, using flight data is graded 4 since no extra sensors are added but the data will give the least amount of information of the proposals. Using IMUs on the landing gear will add sensors and the management of data will be greater than for load cells or strain gauges and is therefore scored lower than these.

With cost efficiency, flight data is given maximum points since no extra component is added and no service cost is expected. Further, IMUs on landing gear require less maintenance and need no calibration and are therefore cheaper to maintain than load cells and strain gauges, which would require high maintenance frequency.

Load cells, strain gauges and IMUs on landing gear were given similar points for system simplicity since sensors will have to be added and they will need wires for connecting them. Using flight data is given a 5 since no sensors are added.

The ease of detection is graded 5 for load cells and strain gauges since the load or strain is measured directly, while it is not for flight data and IMUs on the landing gear. The IMUs on landing gear is graded higher than using flight data since the data will be easier to interpret due to the fact that it is measured on the landing gear. Flight data on the other hand requires a correlation between the aircraft reference frame to the landing gear dynamics.

For maintenance simplicity, the flight data is given the highest score since no additional maintenance will be needed while the IMUs on landing gear will need more maintenance since parts are added. Further, the strain gauge and load cell will need more maintenance since the attachment will degrade over time and recalibration will be needed.

Table 2.4: Flight data parameters available for consideration

Parameter	Unit
Magnetic Heading	Deg
Pitch Angle	Deg
Roll Angle	Deg
Body Pitch Rate	Deg/s
Body Roll Rate	Deg/s
Body Yaw Rate	Deg/s
Body Longitudinal Accel	g
Body Lateral Accel	g
Body Normal Accel	g
Pitch Attitude Rate	Deg/s
Roll Attitude Rate	Deg/s
Yaw Attitude Rate	Deg/s
Vertical Acceleration	g
Along Heading Acceleration	g
Cross Heading Acceleration	g

For fatigue estimation, it will be easiest with the direct measurement that load cells and strain gauges entail, while it will be harder using IMUs and cumbersome modeling with flight data.

2.4 Choice of concept

The results from the weighted decision matrix, see table 2.3, gave an indication of which concept to continue working with. The most promising concept seemed to be using flight data followed by adding IMUs to the landing gear where the flight data got 25 points more. From this, and the indications from the aircraft engineers, the choice was made to continue the work with the flight data. It is possible to include more sensors already existing on commercial aircraft if needed to get a good enough fidelity of the hard landing indication.

The concept was chosen to proceed with, with the intent of creating an algorithm to detect hard landings. The concept may include any combination of the parameters listed in table 2.4 which are commonly recorded in operational aircraft. More inputs than listed in the table are possible to include if it can be proved to increase the reliability of overload detection.

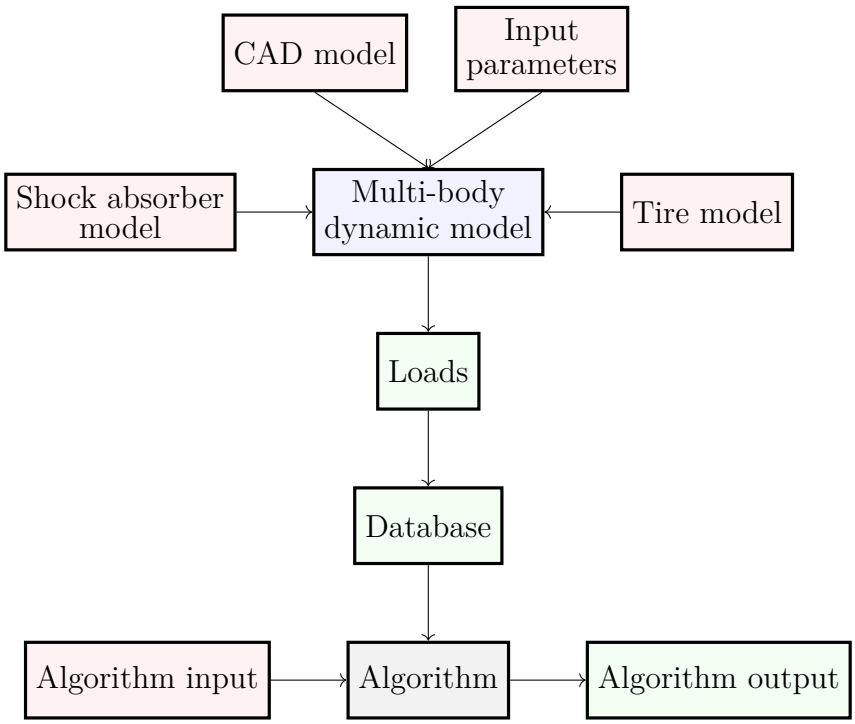

Figure 2.1: Flowchart of the steps to create the algorithm

2.4.1 Description of selected concept

To detect hard landings an algorithm that estimates the forces for a specific landing will be created. The estimation will be performed by comparing the landing scenario to a database of known force results and interpolating between these. The estimated force can potentially be used to check if the landing was a hard landing or not.

2.4.2 Identified steps

For the intended hard landing algorithm to work by assessing forces for a specific landing, a database of known force responses for varying landing scenarios is required. The database will be created by analyzing the dynamic behavior and the forces of the landing gear by multi-body dynamics simulations.

In order to build the multi-body dynamic model used for creating the database, a tire model, shock absorber model and a CAD model of an arbitrary landing gear geometry is needed. These steps are covered in greater detail in the following chapters. A flowchart of the necessary steps can be seen in figure 2.1. 'Input parameters' connected to 'Multi-body dynamic model' represents parameter sets for the landings simulated. The 'Algorithm input' are assumed to already be converted flight data that can be directly used in the algorithm.

3
Geometry and properties

This chapter covers the landing gear geometry, design, materials and resulting landing gear mass as well as assumptions and simplifications made of the landing gear geometry.

3.1 Landing gear geometry

For the design of the arbitrary landing gear, a survey was first performed to find inspiration of landing gear arrangement and dimensions. For an assumed aircraft landing mass of 20 tons, existing aircraft designs indicate a total landing gear mass between 700 kg and 1000 kg. The span is determined from Smith [8, Tab. 13.11] for landing gear masses on aircraft with a total mass between 19 tons and 21 tons.

The general landing gear layout considered is a tricycle layout with two articulated MLGs and a single nose landing gear (NLG), where each landing gear has two wheels. Based on this and the common design practice of a front to rear landing gear mass distribution between 5% and 14%, see Smith [8, p.288], one MLG should be in the range of 301 kg and 475 kg when considering the total landing gear mass span.

3.2 CAD

The software used for creating the CAD model was CATIA V5 [9]. Since the thesis is focusing on a simplified two-point landing through drop test correlation, only the MLG is modeled. Hence, the NLG will not be considered in simulations. The MLG is modeled with a retraction mechanism including a side stay for lateral stability. Illustrations of the MLG design can be seen in figures 3.1 and 3.2.

3.3 Materials and landing gear mass

In order to verify that the design is within the identified mass range, material selection was performed. As common practices and designs that may be found on aircraft in service, material selection of the parts is compiled in table 3.1. Aluminium (AL-7075) is often used in aerospace due to its high strength to mass ratio. Corrosion

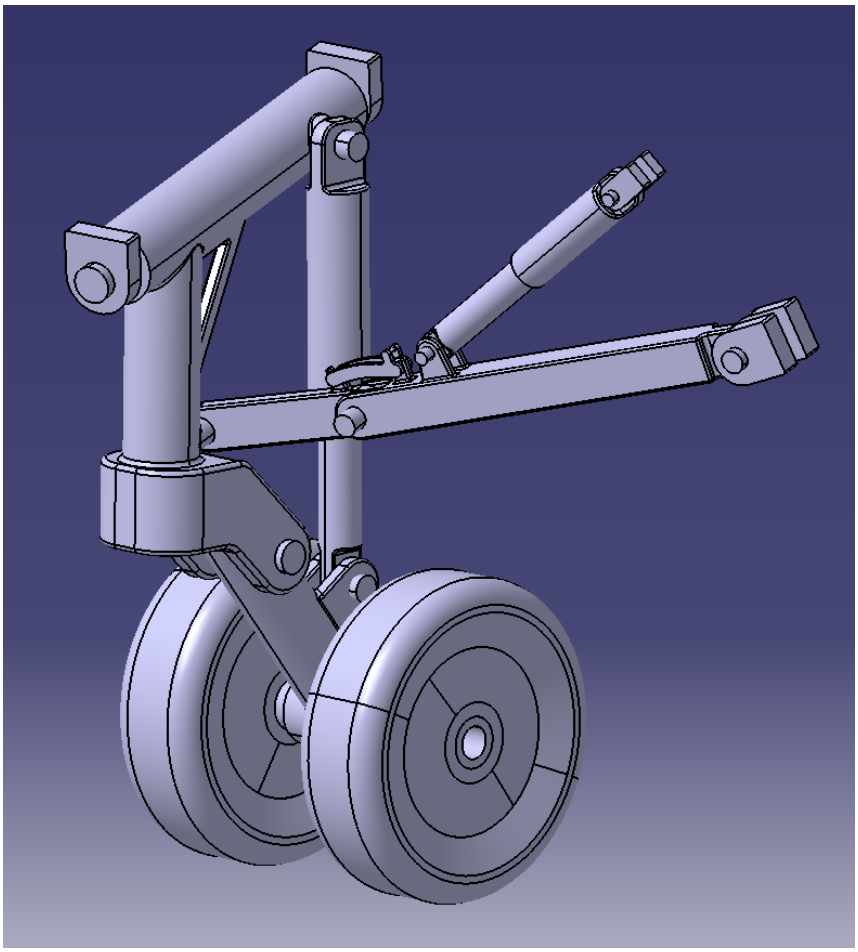

Figure 3.1: CAD of the main landing gear

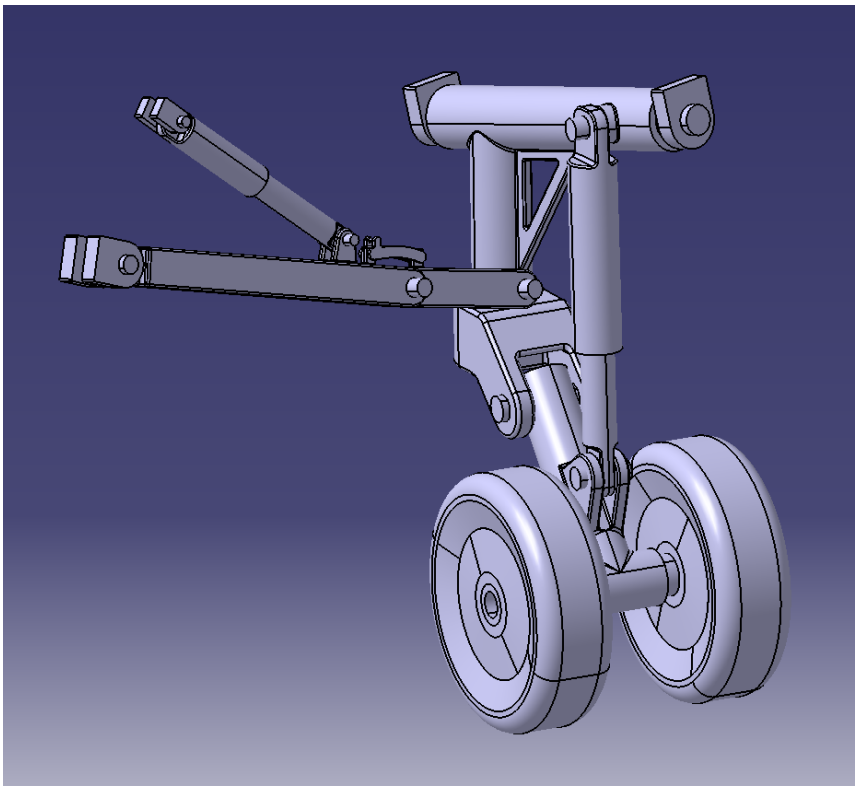

Figure 3.2: CAD of the main landing gear, additional view

Resistant Steel (CRES) is used when necessary and steel (S-4340) where applicable. The same materials were used in multi-body dynamic simulations.

The calculated mass with added materials is 444 kg for one MLG which equals a total landing gear mass of 986 kg if assuming that MLGs constitute 90% of the total mass. This mass is close to the upper boundary of the previously presented identified range. In this calculated mass, wheel and tire masses were assumed as presented in table 3.2, which are based on distribution percentages of the total mass as described by a typical component breakdown in Currey [10, Tab.11.3]. Brake system mass is not considered as separate rotating parts in but is rather included in the modeled CAD parts. Note that 'CAD parts with materials' constitute 71% of total mass due to subtracting the MLG tire and MLG wheel masses from 90%

3.4 Design assumptions and simplifications

In order to make the CAD model within a reasonable time, accounting for that CAD complexity is not the focus of this work, several assumptions were made already during the CAD design which may have effects in simulations. One significant simplification, which will be covered in more detail in the shock absorber modeling chapter, is the choice to not model the shock absorber end stop in CAD but rather by using a shock absorber spring stiffness curve.

Table 3.1: MLG material selection

Part	Material
All pins	S-4340
Cylinder (S/A)	S-4340
Downlock	AL-7075
Leg	AL-7075
Piston (S/A)	S-4340
Retraction cylinder	CRES
Retraction piston	CRES
Side stay lower	AL-7075
Side stay upper	AL-7075
Trunnion	AL-7075
Wheel axle	S-4340

Table 3.2: Wheel and tire masses, including CAD mass for reference

Part	Percentage of total	Mass per MLG
MLG tire	11%	54 kg
MLG wheel	8%	39 kg
CAD parts with materials	71 %	351 kg

Another simplification is that the side stay lock is just geometrically locking the side stay. This means that the lock does not have an actuator for releasing the lock or springs to keep it in place. This was made in order to reduce the complexity of the CAD model since extension and retraction events will not be simulated.

Further, as mentioned the landing gear design is an arbitrary design. This means that the parts modeled have assumed dimensions and follow a novel generic configuration rather than having a very detailed part design. This may have implications for simulation results. Nevertheless, considering that all landing gears are designed for a specific aircraft, variations may be expected. For the rigid body kinematic aspect which is of consideration in the thesis, the implication may be argued to be minimal. This is in contrast to if flexible bodies were to be simulated.

4

Shock absorber model

In order to have the correct behavior in the multi-body dynamic model, a shock absorber model is established to get the spring and damping behavior in the landing gear.

4.1 Theory

This section covers the theoretical background employed for the shock absorber behavior.

4.1.1 Flow rate through an orifice

The flow rate (volume per time) through a single orifice can be described as

$$Q = A_{effective}\sqrt{\frac{2|p_u - p_d|}{\rho}}\, sgn(p_u - p_d) \tag{4.1}$$

where Q is the flow rate through the orifice, $A_{effective}$ is the effective area of the orifice, p_u is the upstream pressure, p_d is the downstream pressure and ρ is the fluid density, see Smith [8, p.373].

4.1.2 Effective area

The effective area, $A_{effective}$ is the reduced area which the fluid may pass through due to the viscosity of the fluid. The relationship between the true area and the effective area is

$$A_{effective} = C_d A \tag{4.2}$$

where C_d is the discharge coefficient and A is the true area of the orifice [8, p.373].

4.1.3 Pressure relation Adiabatic process

The relation between pressure and volume at two instances in an adiabatic process can be described as

$$P_1 V_1^{\gamma} = P_2 V_2^{\gamma} \tag{4.3}$$

where P_1 is the pressure and V_1 is the volume at the first instance, P_2 is the pressure and V_2 is the volume at the second instance and γ is the polytropic coefficient, see Smith [8, p.406].

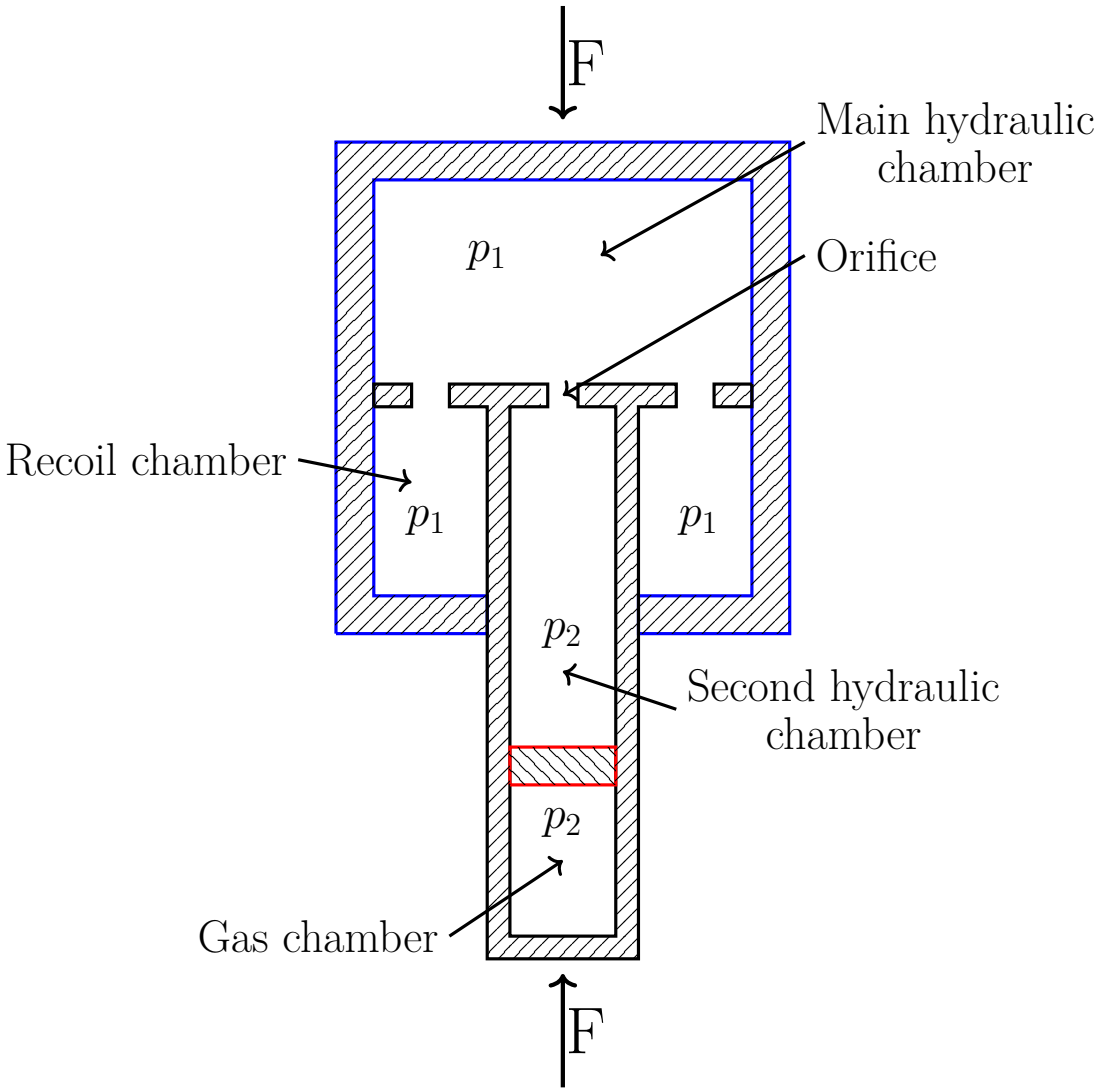

Figure 4.1: Cross section view of the shock absorber and the loads acting on it. The cylinder is blue, the piston is black and the floating piston is red.

4.2 Method

The section describes the method related to the shock absorber.

4.2.1 Shock Absorber Force

The shock absorber is a simple arbitrarily chosen shock absorber and the loads acting on the shock absorber can be seen in figure 4.1. From force equilibrium of the piston head in axial direction, in a time instance, the following equation can be established:

$$F = p_1 A - p_1(A - A_p) = p_1 A_P \tag{4.4}$$

where the friction has been neglected and A_P is the piston area. The volumetric flow rate from the cylinder is equal to the volumetric flow rate through the orifice

and secondary hydraulic chamber. The volumetric flow rate through the orifice can therefore be described as:

$$Q_{orif} = \dot{S}A - \dot{S}(A - A_p) = \dot{S}A_p \tag{4.5}$$

where $\dot{S}$ is the relative velocity between the piston and cylinder. The flow through the orifice can also be described from Eq. (4.1) together with Eq. (4.2) as

$$Q_{orif} = C_d A_{orif} \sqrt{\frac{2\Delta p}{\rho}}. \tag{4.6}$$

By substituting Eq. (4.6) into Eq. (4.5) an equation of the pressure difference upstream and downstream of the orifice can be obtained as

$$\dot{S}A_p = C_d A_{orif} \sqrt{\frac{2\Delta p}{\rho}} \implies \Delta p = \left(\frac{A_p}{C_d A_0}\right)^2 \frac{\rho}{2} |\dot{S}|\dot{S}. \tag{4.7}$$

Now substituting in Eq. (4.7) into (4.4), the shock absorber force becomes

$$F = \frac{A_p^3}{(C_d A_0)^2} |\dot{S}|\dot{S} + p_2 A_p. \tag{4.8}$$

The pressure p_2 can be described with the pressure from the gas chamber onto the floating piston that separates the oil from the gas. Here it is assumed that the pressure on both sides of the piston will be the same. Using Eq. (4.3) with $V_1 = V_0$, $P_1 = p_{ao}$ and $V_2 = V_0 - A_p S$ with S as the stroke, p_2 can be described as

$$p_2 = p_{a0} \left(\frac{V_0}{V_0 - A_p S}\right)^{\gamma}. \tag{4.9}$$

Substituting Eq. (4.9) into (4.8) gives the final equation of the shock absorber force as

$$F = \frac{\rho A_p^3}{2(C_d A_0)^2} |\dot{S}|\dot{S} + p_{a0} A_p \left(\frac{V_0}{V_0 - A_p S}\right)^{\gamma}. \tag{4.10}$$

The force can be separated into a damper force and spring force as:

$$F = F_{damper} + F_{spring} \tag{4.11}$$

$$F_{damper} = \frac{\rho}{2(C_d A_0)^2} A_p^3 |\dot{S}|\dot{S} \tag{4.12}$$

$$F_{spring} = p_{a0} A_p \left(\frac{V_0}{V_0 - A_p S}\right)^{\gamma} \tag{4.13}$$

4.2.1.1 Shock absorber parameters

The shock absorber parameters are chosen based on typical values and tuning of the parameters in the drop test described in Chapter 5 and can be seen in table 4.1. The oil density is dependent on pressure and temperature but was approximated to 860 kg/m^3 through the whole process. D_p and S_{max} were chosen to be similar to

the arbitrary landing gear described in Chapter 3. p_{a0} was chosen based on similar aircrafts and γ is typically 1.35 [8, p.407].

From the stroke, initial pressure and maximum pressure the initial gas volume V_0 could be calculated from Eq. 4.3 as

$$V_0 = \frac{A_p S_{max} p_2}{p_2 - p_{a0}} \tag{4.14}$$

with $\gamma = 1$ since the maximum pressure was based on the isothermic load case of a 1.7g bump which gave a pressure of $p_2 = m_{AC} \cdot 1.7g/A_p$.

C_d is usually in the span between 0.65 to 0.97 [8, p.374] and a C_d in the span between 0.7 and 0.8 seemed reasonable. A more exact number was investigated during the drop test simulation where also an estimation of the orifice diameter D_0 was done.

Table 4.1: Shock absorber parameters

Parameter	Value	Unit	Explanation
m_{AC}	10	ton	Half aircraft mass
ρ_{oil}	860	kg/m^3	Density of the oil
C_d	0.8	–	Discharge coefficient
D_0	9	mm	Orifice diameter
D_p	95	mm	Piston outer diameter
p_{a0}	22.5	bar	Initial air pressure
V_0	$1.48 \cdot 10^6$	mm^3	Initial air volume
γ	1.35	–	Polytropic coefficient
S_{max}	189	mm	Maximum stroke

4.2.2 Bottoming

In order to model bottoming and maximum extension, a very high force per stroke was added to the spring curve at $-1 < S < 0$ mm and $189 < S < 190$ mm. This was done instead of creating the CAD details required and implementing a contact formulation in the multi-body dynamic simulations. This corresponds to a penalty formulation for contact. The force vs stroke of oil is approximated to be linear between $0 < S < 2$ mm since the compressibility of oil is very small compared to air.

4.3 Result

The spring force curve F_{spring} can be seen in figure 4.2 and the damper force curve F_{damper} in figure 4.3. The spring curve including the bottoming loads, which is the spring curve implemented to the multi-body dynamic model, is seen in figure 4.4.

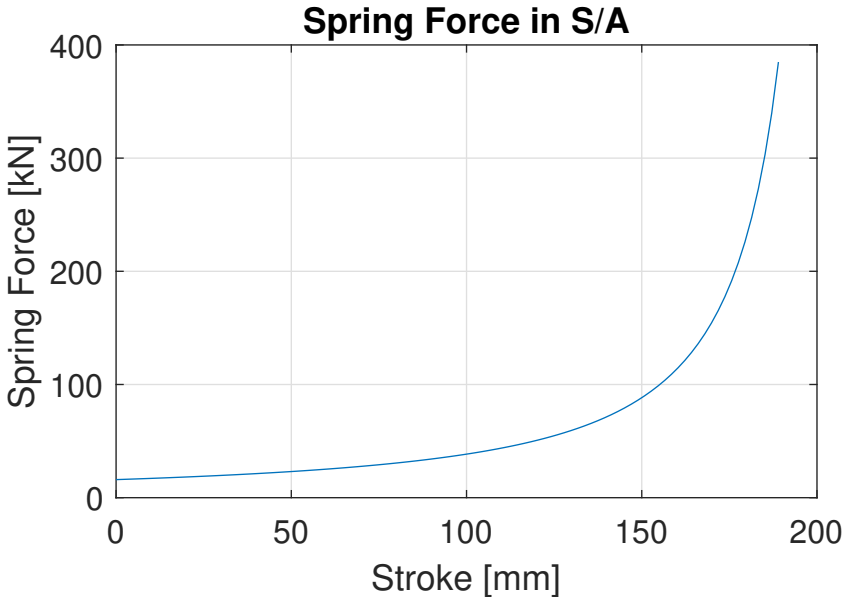

Figure 4.2: Spring force, F_{spring} vs Stroke

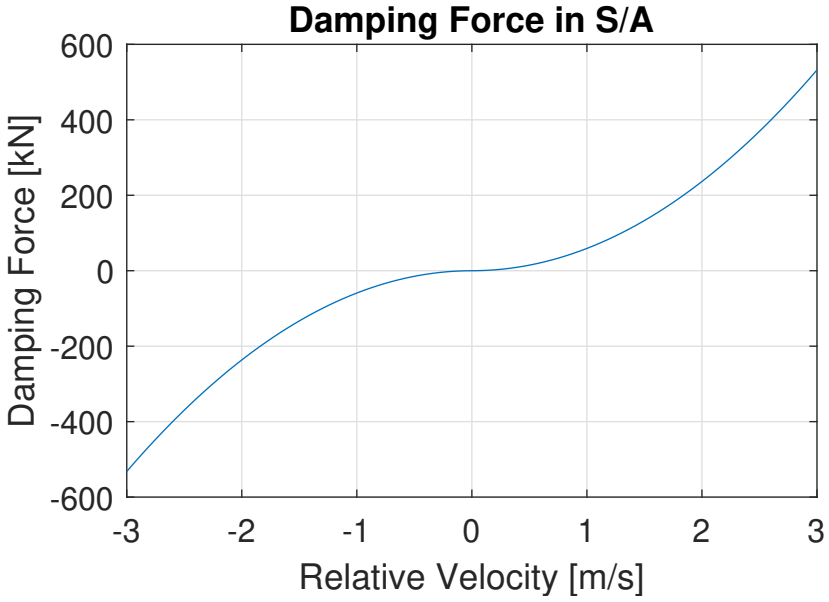

Figure 4.3: Damper force, F_{damper} vs relative velocity

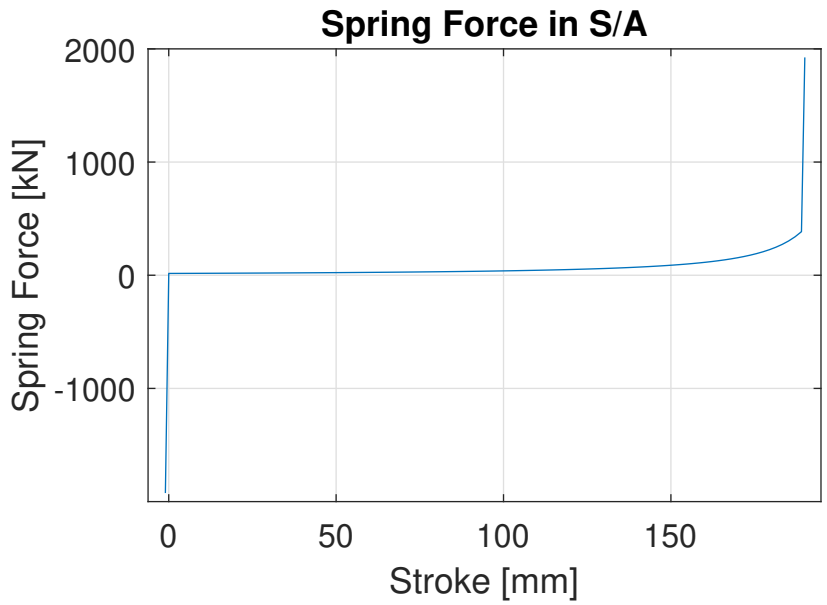

Figure 4.4: Spring force, F_{spring} vs Stroke including artificial stops and compression of oil.

4.4 Simplifications and the impact of them

Having the same shock absorber force curve for both compression and extension of the shock absorber is not true in practice. There is usually some hysteresis in the spring and damper curve because of friction in the bearings and seals of the shock absorber and the temperature change in the system. Even though a real case scenario will not be achieved, the simplification to use the same shock absorber curve for both compression and extension is good enough since the purpose of the model is to be used as a tool to detect loads and not to model the perfect behavior of the shock absorber.

5

Multi-body dynamics model

In order to relate the flight data parameters to loads on the landing gear tire contact patch, a multi-body dynamic model was built. The model represents a drop test simulation where several parameters were varied to determine the influence of each parameter on the loads. A reduction of the possible landing cases is thus made by exclusively considering a drop test model, however, an initial evaluation of the concept may still be made from this.

5.1 Creating the model

The multi-body dynamic model was built using MSC Adams [11], a multi-body dynamics simulation tool commonly used for various dynamic simulations including landing gear analysis. MSC Adams uses an implicit method to solve non-linear differential equations, see Adams solver default settings in Adams help documentation [11].

Pre-processing of the model entailed importing the CAD geometry and constraining the parts. Materials were assigned according to table 3.1 for mass and inertial properties and the wheels were given masses according to table 3.2 and inertial data estimated from the CAD model. Further, a ground contact plane was created and a point mass representing an aircraft drop mass was added which the gear was constrained to. The drop mass was constrained to only allow vertical translation to mimic a drop test. The shock absorber model previously created was also imported to Adams and a tire model was chosen with tire data as is discussed in subsection 5.1.1 below.

The Adams model can be seen in figure 5.1 where the red sphere represents the drop mass. Relevant constraints are presented in table 5.1. A simplification was made for the wheel to wheel axle joints, where it was assumed that there is no friction. The result of this is that the longitudinal force on the tire contact surface was slightly larger. But it also meant that the initial condition set to the wheel angular velocity was valid when the tire contacted the runway regardless of the different drop heights simulated. As such, no consideration needed to be taken to different times passing before tire and ground contact, otherwise resulting in different reductions of the angular velocity during the drop.

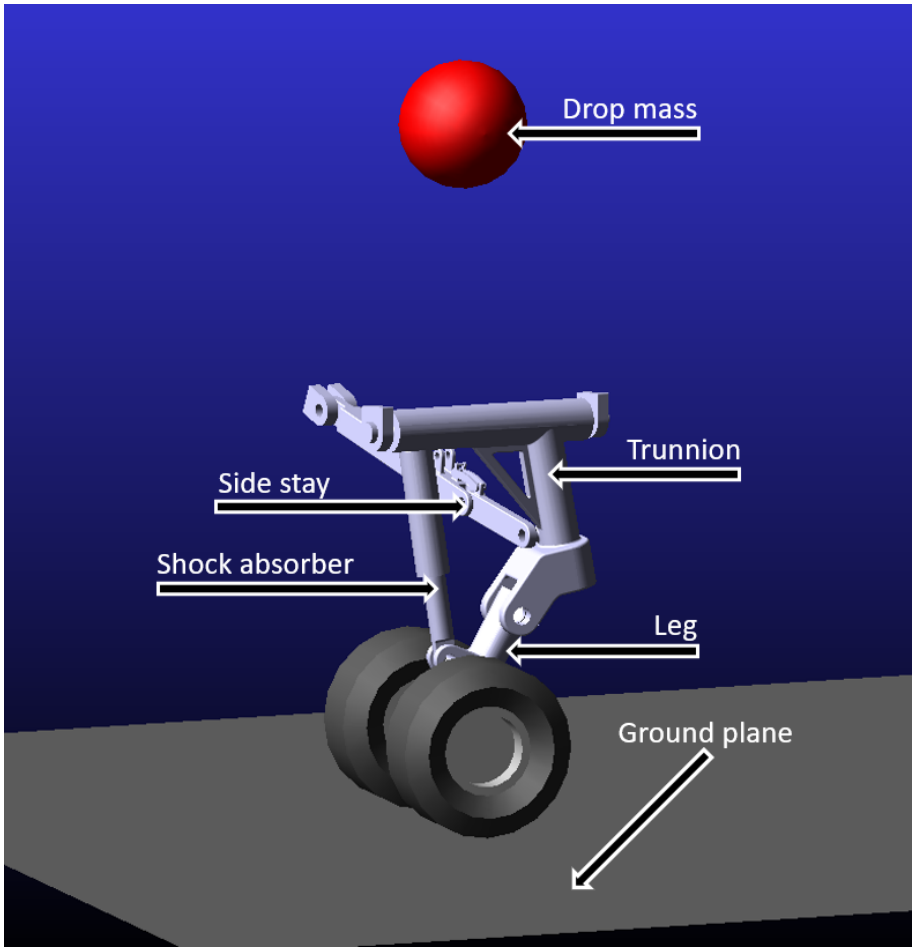

Figure 5.1: Adams drop test model set up

Table 5.1: Constraints in the MLG model

ID	Part 1	Part 2	Connection
1	Drop mass	Mounts	Fixed
2	Mounts	Trunnion	Hinged
3	Mounts	Side stay upper	Hinged
4	Trunnion	Leg	Hinged
5	Trunnion	Cylinder	Hinged
6	Trunnion Pin	Fuselage attachment	Hinged
7	Piston	Cylinder	Prismatic
8	Leg	Piston	Hinged
9	Leg	Wheel axle	Fixed
10	Wheel axle	Wheel	Hinged
11	Side stay upper	Side stay lower	Hinged
12	Side stay lower	Trunnion	Hinged

Table 5.2: Tire data for H27x8.5-14

Parameter	Value	Note
Radius	13.5 inch (0.343 m)	-
Width	8.5 inch (0.216 m)	-
Rim radius	7 inch (0.178 m)	-
Rated max load	13300 lb (6033 kg)	-
Rated pressure	207 psi (14.3 bar)	Also used for inflation pressure
Static rated load radius	11.4 inch (0.290 m)	2.1 inch deflection from unloaded
Vertical damping	6.3 lbs/inch (1100 Ns/m)	1/1000 of vertical stiffness [11]
Bottoming radius	7 inch (0.18 m)	Assumed from similar tires
Friction, max	0.8	Static friction, regulated [7]
Velocity, reference friction	1000 inch/s (25.4 m/s)	At which 36% of max applies, for determining friction decay

5.1.1 Tire modeling

The Adams TRR64 tire model was used [11, TRR64 tire model], which has been created specifically for aircraft tires and is a basic version of NASA TR-R64 on aircraft tire mechanical properties, see Smiley & Horne [12]. For tire data, Michelin Aircraft Tire Engineering Data [13] was used, specifically Michelin H27x8.5-14. Relevant parameters extracted from the datasheet for this tire can be found in table 5.2. Other types of possible tire selections can be found in Goodyear Aviation Tire Data Section [14] and more information on aircraft tires in general and practice can be found in Dunlop Aircraft Tire General Practices [15].

The tire stiffness is calculated in the TRR64 model automatically, however for determining the vertical damping, the vertical tire stiffness was estimated by the rated load divided by the difference between the unloaded and rated load radius. Vertical damping was then calculated as approximately 1/1000 of the vertical tire stiffness, defined in Adams help documentation [11, TRR64 tire model]. For the bottoming radius, since no value is entered for Michelin H27x8.5-14 in the tire data, a value was assumed from similarly sized tires in [13][14]. The tire characteristics for a bottoming case are handled by the tire model, specifically by a significant increase in vertical stiffness. This bottoming stiffness curve can be manipulated, but the standard values were kept.

Specific for the TRR64 model is the selection of 'Handling Mode' and 'Friction Mode' where options 'Simple NASA TR-R-64' and 'Slip Velocity based Model A' were used respectively. The Simple NASA TR-R-64 Handling Mode is the standard simplified interpretation of the model and is thus chosen. Slip Velocity based Model A Friction Mode is a decaying friction model, where the friction coefficient tends towards zero for increasing slip velocity. A slip velocity to obtain a reference friction was thus needed, and the value in table 5.2 was kept as standard in the model. For further information and comparison with other types of handling and friction modes, see Adams help documentation [11, TRR64 tire model].

5.1.2 Drop test

First, the drop test model was used to verify the tire and shock absorber behavior to what can be expected in a real drop test. An actual drop test is performed by constraining a landing gear in a rig which drops from a specific height to reach a certain vertical velocity upon contact with the ground. As such, in the model, the point mass was constrained such that it only allowed translation in vertical direction and the only applied load was the drop mass corresponding to the aircraft mass. However, the drop mass was reduced to half of the aircraft mass, since this is what would be acting on each landing gear.

Moreover, since the lift force reduces the total vertical load a so called equivalent weight was implemented. The equivalent weight was calculated according to ARP5644 [16, sec. 12.2] as

$$W_e = W \frac{h + (1 - L)d}{h + d} \tag{5.1}$$

where d is the maximum vertical travel distance of carriage after the tire has made contact with the ground, h the theoretical free drop height, L the aircraft lift to weight ratio (set to 1 for drop test, which is the highest value it may have). The equivalent weight W_e was thus reduced from the true aircraft weight W, in this case corresponding to a mass of 10 tons for one MLG.

The free drop height was determined by energy equilibrium according to

$$mgh = \frac{mv^2}{2} \implies h = \frac{v^2}{2g} \tag{5.2}$$

where a sought vertical velocity of 3 m/s (10 ft/s, see section 5.2.1) resulted in $h =$ 458 mm. The distance d was initially estimated in order to obtain a first guess of the equivalent weight. The calculated equivalent weight includes the landing gear, but as the landing gear mass was included in the model, this was subtracted to get the value to apply to the drop mass.

The initial guess of d = 300 mm consisted of 200 mm vertical (wheel) axis travel (VAT), and 100 mm tire deflection. With this guess, W_e corresponded to 6042 kg, including the landing gear mass. When the drop test simulation was run with this value it showed a maximum d = 285 mm, whereby the equivalent weight was updated to W_e corresponding to 6164 kg. With this equivalent weight, a maximum d = 289 mm was obtained. This was deemed to have converged since it was a change of 1.4 %.

In order to allow further intended use, the wheels were assigned a design variable to change the initial condition of angular velocities. This to mimic longitudinal velocities and to capture spin-up and spring-back phenomenons. This approach was chosen since the landing gear or ground is not translating longitudinally. Further design variables were added in Adams to easily edit the drop height and drop mass,

Table 5.3: Design variables in drop test model

Design variable	Expression & Unit	Comment
Drop mass, m_{drop}	Input [kg]	Excluding MLG mass
Vertical velocity, v_z	Input [m/s]	Linked to drop height
Drop height, h	$\frac{v_z^2}{2g}$ [m]	-
Heading velocity, v_x	Input [m/s]	Linked to angular velocity
Angular velocity, ω	$\frac{v_x}{R_{tire}}$ [rad/s]	R_{tire} unloaded tire radius [m]

Table 5.4: Batch run input parameters with ranges and increment sizes

Parameter	Lower limit	Upper limit	Increment size
Pitch, θ	1°	11°	2°
V_z	1.0 m/s	4.0 m/s	0.5 m/s
ω_{wheel}	-200 rad/s	-100 rad/s	20 rad/s
W_e	1000 kg	8500 kg	750 kg

such that batch runs could be performed. The design variables are compiled in table 5.3.

5.2 Parameter sweep batch runs

A requirement for creating the algorithm was building a database of simulation results. This database was obtained by performing batch runs where the design variables were varied by parameter sweeps. As such, large amounts of data were collected from the drop test model. The parameters that were swept over were vertical velocity, longitudinal velocity (represented by wheel angular velocity), aircraft pitch angle and equivalent weight. The sweeps were performed by varying vertical velocity, wheel angular velocity and drop mass for each specific batch. Each batch was simulated for every pitch angle, which was varied by manually rotating the landing gear without parameter involvement.

The batch runs were scripted using Python and the script was imported to Adams for each pitch angle. The simulation results of forces acting on the tire, wheel angular velocities and displacements (d) were saved for later use. From the force results, Pareto surfaces were created for each pitch angle and vertical velocity combination, such that the forces could be visualized in three-dimensional plots. An example of one of the Pareto surfaces can be seen in figure 5.3 in the Adams result section 5.3. The batch run input ranges and increment sizes are compiled in table 5.4, but are also explained briefly in the following sections.

5.2.1 Varying vertical velocity

Vertical velocity is one of the most critical parameters driving the loads in the landing gear. The chosen range of vertical velocities was between 1.0 m/s and

4.0 m/s, as it was assumed that landings below 1.0 m/s are rare and not critical. According to regulations [7, CS 25.473 (2)] a vertical velocity higher than 3.0 m/s (10 ft/s) with designed landing mass is traditionally deemed a hard landing. The upper limit of 4.0 m/s was thus chosen to ensure landings above the traditional limit can be tested, however, extreme landings above 4.0 m/s may be argued should lead to AoG or inspection regardless.

5.2.2 Varying wheel angular velocity

The wheel angular velocity was varied between 100 rad/s and 200 rad/s in reverse direction. This corresponds to a longitudinal velocity between 34.3 m/s and 68.6 m/s for an unloaded tire radius of 0.343 m. The limits were taken from nominal stall velocities and maximum landing velocities, see [17, Aircraft category A & B].

5.2.3 Varying pitch angle

The pitch angle was varied between 1 degree and 11 degrees rearward in 2 degree increments. The lower limit was set since 0 degree pitch equates to a three point landing, no longer represented by a drop test. For pitches higher than 11 degrees the risk of tailstrike may be imminent depending on specific aircraft design and is thus not relevant. As an example, a Boeing 747-400 has a tailstrike angle at 12.5 degrees [18, Fig. 1] and a Boeing 777-300ER a tailstrike angle at 10 degrees [19].

5.2.4 Varying mass

Since flights are performed with different masses based on the number of passengers and luggage as well as varying fuel usages, the mass was also varied as an input parameter. The mass variation was performed by the equivalent weight added to the drop mass in Adams. Since the true weight is a function of the equivalent weight W_e, free drop height h and carriage travel distance d, a specific equivalent weight does not equal the same true weight for all other parameter variations.

As such, for each drop test simulation in the batch runs, the true weight for that simulation was calculated based on input W_e, h and resulting d. As previously mentioned the lift to weight ratio $L = 1$ was used for all drop tests. The range of true weight was for masses between an upper value of 11 tons as a margin of the maximum take-off mass (MTOM) of 10 tons considered in the thesis, and a lower value at 80% MTOM, 8 tons, as an assumed design landing mass. The equivalent weight was varied in a large enough range to ensure data for the sought true weight for all batch runs. The lower limit for equivalent weight was for a mass of 1000 kg whereas the upper limit was for a mass of 8500 kg. Both limits were found by testing extreme cases of parameter combinations in the model and calculating the true weight for those.

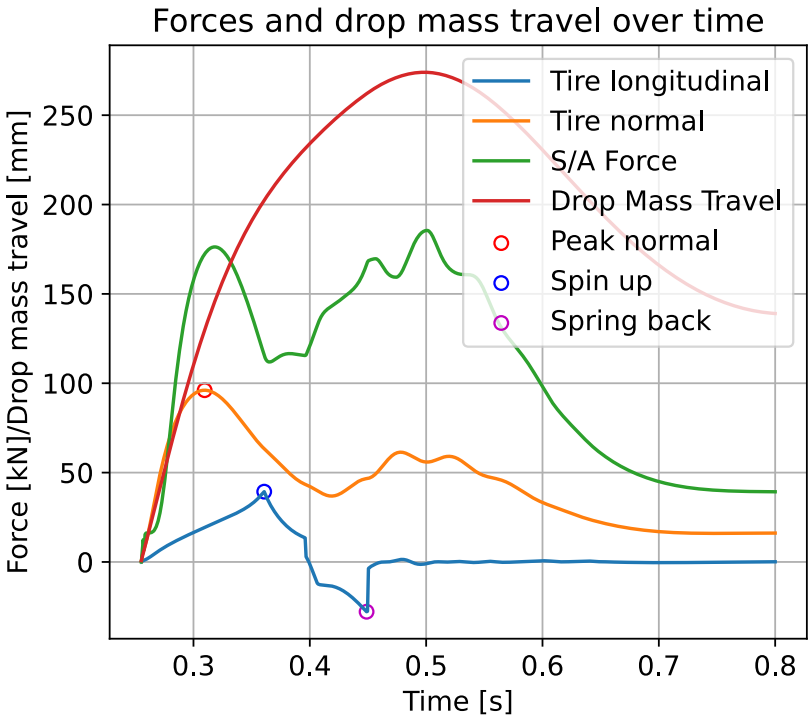

Figure 5.2: Tire forces, shock absorber force and drop mass travel vs time with $\theta = 5$ degrees, $v_z = 2.5$ m/s, $\omega = -120$ rad/s and $W_e = 5944$ kg

5.3 Adams simulation results

Results from the multi-body dynamic model are presented and interpreted next, both a single drop test example as well as a batch run example.

5.3.1 Single drop test simulation

An illustration of an example of the results during a drop test simulation can be seen in figure 5.2. The figure shows the tire normal force, tire longitudinal force, shock absorber force and drop mass travel distance, d. The tire normal force peak seen in the figure occurs at the beginning of the landing. It occurs because of the high velocity which is dampened by the shock absorber which induces the peak force through the shock absorber and tire. The longitudinal force in the tire patch will be increased until the tire is up to speed with the aircraft which is called spin up. After the spin up, the force is reduced and its lower peak, called spring back, occurs when the energy stored in the tire and structure is released which causes a movement of the tire in the opposite direction [8, p.813].

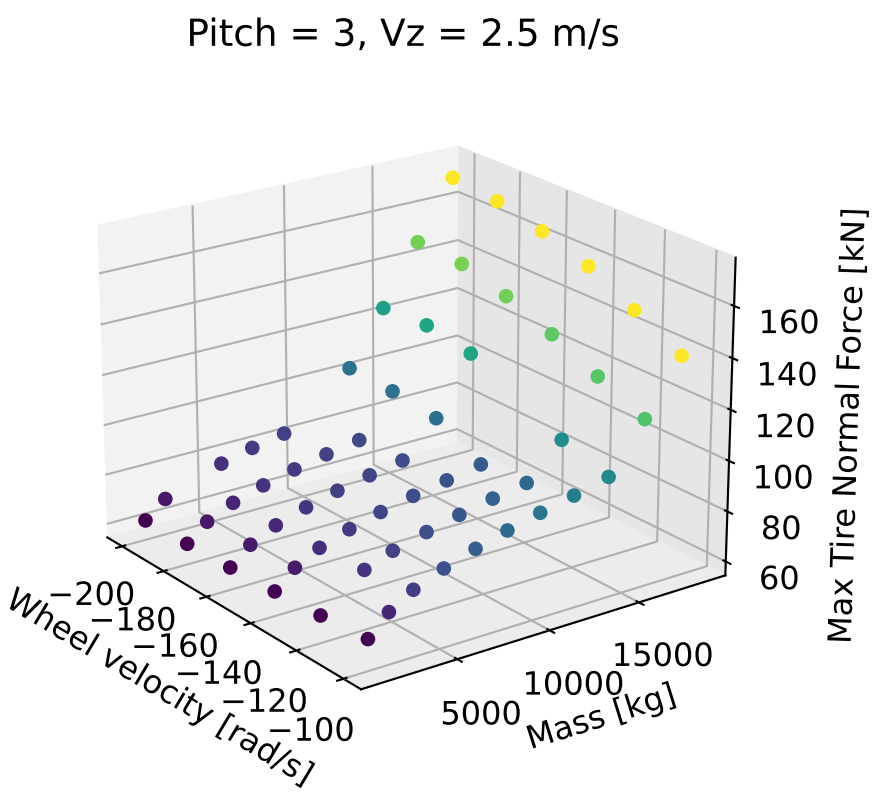

Figure 5.3: Maximum Tire Normal Force Pareto surface plot for batch run at pitch = 3 degrees, plotted for all simulations at $v_z = 2.5$ m/s

5.3.2 Batch run simulations

The batch runs of the drop test model result in a database which can be illustrated for a specific pitch angle and vertical velocity as a Pareto surface in a three dimensional plot. An illustration of one of the solution surfaces can be seen in figure 5.3. The in plane axes are for wheel velocity and true drop mass whereas the out of plane axis is the force, in this case, the maximum tire normal force. Some data points are missing on the surface because some of the simulations failed when the batch runs were performed. A noticeable increase in the force can be seen for the higher masses, which is due to the shock absorber bottoming and resulting in higher peak forces in the tire normal direction. An illustration of the tire longitudinal force for the same batch can be seen in figure 5.4.

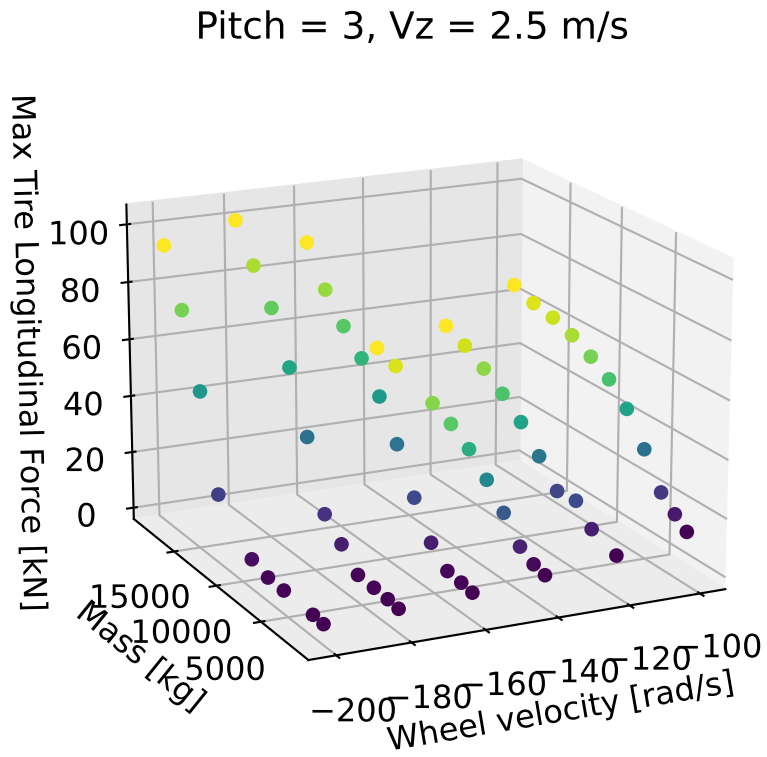

Figure 5.4: Maximum Tire Longitudinal Force Pareto surface plot for batch run at pitch = 3 degrees, plotted for all simulations at $v_z = 2.5$ m/s

6
Creating an algorithm

The final algorithm for hard landing detection is here covered in detail regarding input, functionality and output. Several steps of evaluating the algorithm are presented, and the results of the algorithm prediction are covered. In this chapter, it is assumed that the created models are valid.

6.1 Algorithm structure

The algorithm estimates the tire normal and longitudinal peak forces for a landing event. It has several parameters for a moment prior to landing as initial conditions and uses a database of known tire forces for a set of input parameters. These tire forces are interpolated based on the input parameters to perform the estimation.

6.1.1 Inputs

The input parameters are converted from the flight data. The conversion is not a part of the thesis but is discussed in section 8.2. The input parameters are presented in table 6.1. Note that the range of the wheel angular velocity used in the batch run simulations corresponds to longitudinal velocities between approximately 35 m/s and 70 m/s with an unloaded tire radius of 0.343 m. In the batch runs, parameters were as previously stated varied for nominal landing ranges discretely to cover the expected values of input parameters. Based on the variations of the simulations the algorithm has limits of inputs for which it can make tire force estimations. The algorithm limits are also included in table 6.1.

6.1.2 Output

The algorithm output is mainly focused on the tire normal force and tire longitudinal force but also the combined magnitude of these. These forces are estimated at three

Table 6.1: Input parameters with ranges and resolutions

Parameter	Lower limit	Upper limit
Pitch, θ	1°	11°
V_z	1.0 m/s	4.0 m/s
V_x	35 m/s	70 m/s
m	8000 kg	11000 kg

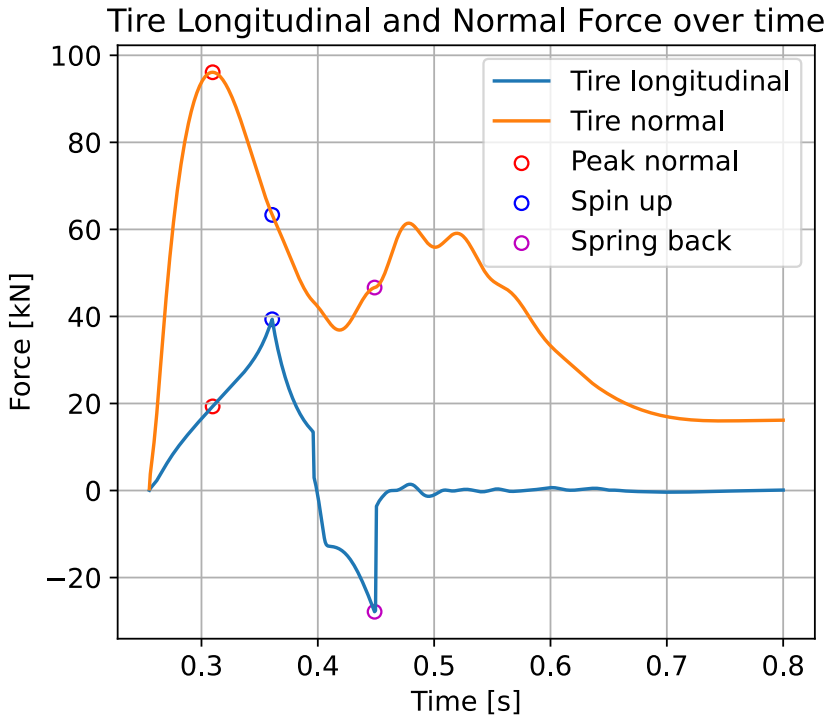

Figure 6.1: Simulated tire forces vs time and the 3 critical instances, for pitch= 5 degrees, $v_z = 2.5$ m/s, wheel velocity= -120 rad/s and equivalent mass= 5944 kg

instances in time where critical loads could occur. One of the instances is the peak tire normal force. Another instance, called spin up, is when the tire longitudinal force is at its maximum. There is also an instance when the tire longitudinal force is at its minimum, called spring back. The instances for one simulation can be seen in figure 6.1.

An example of the output of the algorithm, for a set of input parameters, can be seen in figure 6.2. The continuous lines are the exact forces and the dots are estimated forces from the algorithm.

6.1.2.1 Overload statement

In order to have the algorithm output as a binary yes or no statement to whether an overload occurrence was noted for a specific landing, the estimated loads would need to be checked against threshold loads. The checks would be performed for the individual force components and the combined force vectors.

Since it is of interest to give an overload statement based on stresses in the landing gear but the thesis does not cover any stress analysis, threshold loads are not considered. The thresholds would need to be based on the structural response of the landing gear based on applied loads in varying directions.

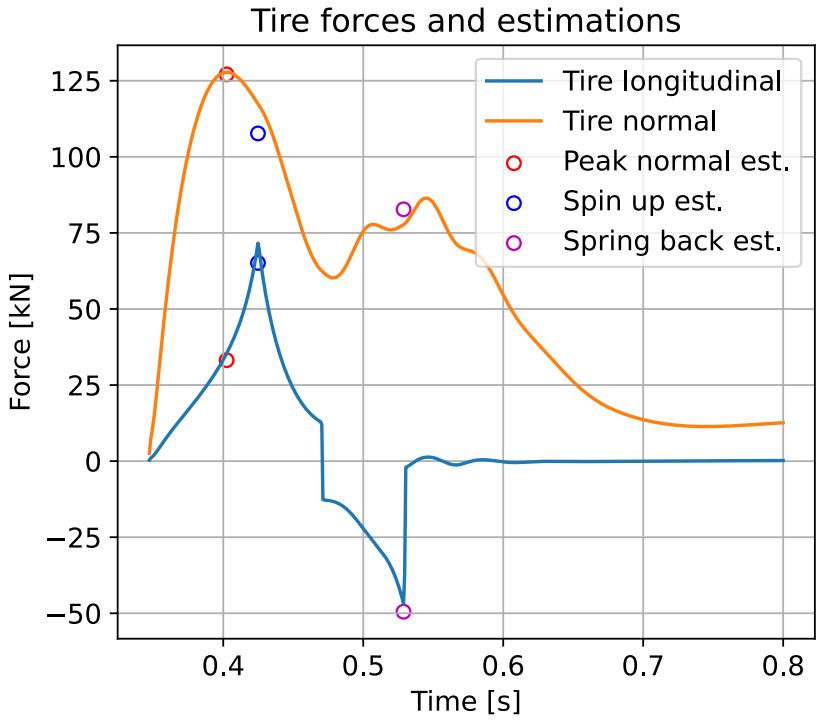

Figure 6.2: Estimation of the tire longitudinal and normal force at critical instances. F_L is the longitudinal force and F_N the normal force.

6.1.3 Structure

The algorithm takes the inputs from a landing and locates the upper and lower values in the database. These values are the tire normal and tire longitudinal forces as well as the true mass, corresponding to the true weight, for each data point. In total 16 data points are found, where the parameter combinations branch out as illustrated in figure 6.3.

The forces extracted from the database are then linearly interpolated based on first the aircraft mass, followed by the longitudinal velocity, vertical velocity and lastly the pitch angle. The longitudinal and normal forces at the three critical instances of a landing are thus obtained and an overload statement can in theory be issued if comparisons of the forces to certain thresholds are made. A flow chart of the algorithm can be seen in figure 6.4 and a pseudo code of the algorithm is presented in algorithm 1.

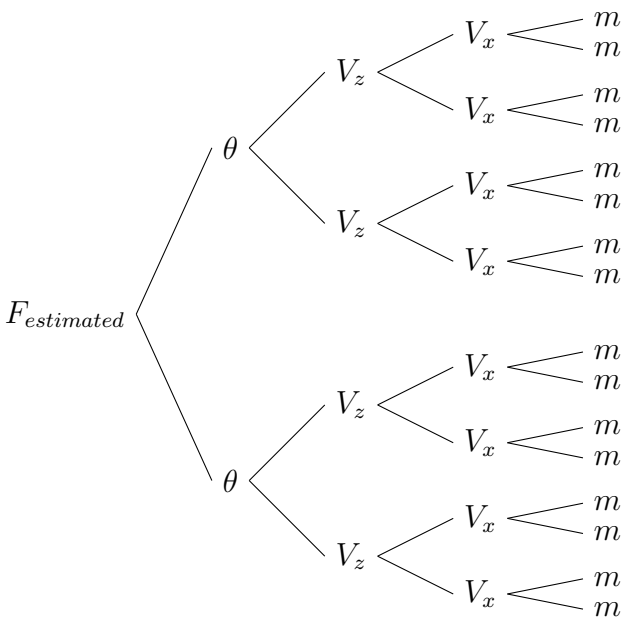

Figure 6.3: Parameter interpolation order branch

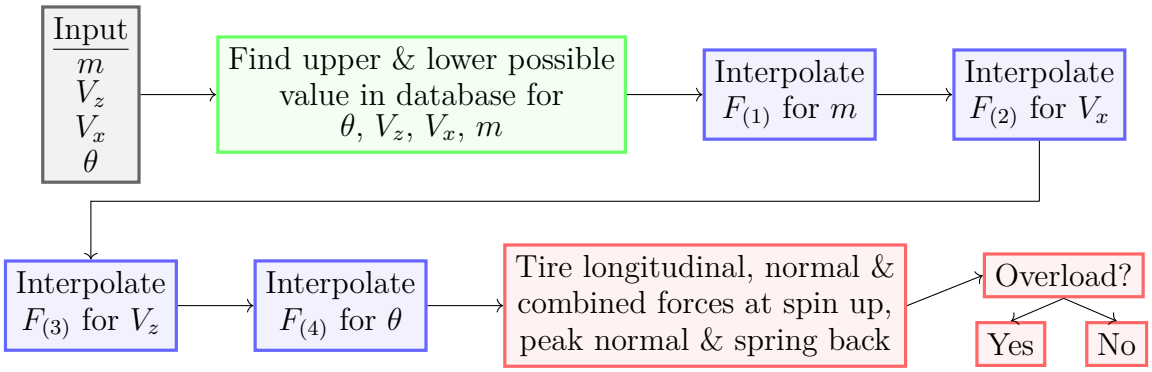

Figure 6.4: Flow chart of algorithm functionality

Algorithm 1 Pseudo code

Input θ V_z V_x m $F_{database}$
Output F
θ_{upper}, θ_{lower} ← possible database upper & lower θ of θ
$V_{z,upper}$, $V_{z,lower}$ ← possible database upper & lower V_z of V_z
$V_{x,upper}$, $V_{x,lower}$ ← possible database upper & lower V_x of V_x
for $\theta_{upper}, \theta_{lower}$ **do**
  for $V_{x,upper}, V_{z,lower}$ **do**
    for m_{upper}, m_{lower} **do**
      $V_{x,force}$ append Interpolated $F_{database}$ based on m, m_{upper}, m_{lower} at the 3 instances
    end for
    $V_{z,force}$ append Interpolated $V_{x,force}$ based on V_x, $V_{x,upper}$, V_{x_lower}
  end for
  θ_{force} append Interpolated $V_{z,force}$ based on V_z, $V_{z,upper}$, $V_{z,lower}$
end for
F ← Interpolated θ_{force} based on θ, θ_{upper}, θ_{lower}

Table 6.2: Input parameters used for validation

Parameter	Validation set
Pitch, θ	[1, 2, 3, 4, 5, 6, 7, 8, 9]°
V_z	[1.0, 1.8, 2.7, 3.4] m/s
V_x	[39, 54, 59, 61.7] m/s
$m(W_e)$	[1257, 4200, 5760, 7503] kg

6.2 Evaluating the algorithm

Evaluation of the algorithm functionality was performed in several steps. First, the interpolation aspect was validated, followed by a sensitivity analysis of runway friction which is assumed as described in section 5.1.1, and knowledge of shock absorber servicing state.

6.2.1 Validation

Validation of the algorithm functionality and results was performed by running more simulations of the multi-body dynamic model with other parameter inputs than those used in the batch runs. The validation parameter inputs were also used as inputs to the algorithm, and the output forces were compared with the exact solutions from the multi-body dynamic model. The set of parameters used for validation can be seen in table 6.2.

It is important to note that in the validation runs where the resulting true mass was outside the defined boundaries between 8 tons and 11 tons, the results were not used for validation since the algorithm is not expected to function outside the limits. While batch run data exist for some values outside, it is not guaranteed and the

Table 6.3: Errors for different forces at spin up instance

	Mean error	Largest error	Smallest
Tire Normal	7.62%	42.2%	0.01%
Tire Longitudinal	6.10%	21.9%	0.01%
Tire Magnitude	6.92%	34.8%	0.04%

batch run results are not expected to be correct since the landing gear is designed for certain masses.

The tire longitudinal and normal forces at the three instances can be seen in figures 6.5, 6.6 and 6.7, where the forces are sorted from minimum to maximum exact force for each instance separately. For the force magnitudes, see appendix A.1, A.2 and A.3. The longitudinal force is sorted independently of the normal force which means that the tire's normal force at a certain x-axis 'data point' does not necessarily correspond to the same 'data point' for the longitudinal force.

The main values considered were the errors, calculated as percentage differences between the validation simulations forces and the algorithm estimated forces. The largest error, smallest error and the mean of all errors were considered, for both vertical and longitudinal forces and the force magnitude separately.

The results show that the estimated forces are following the same trend as the exact forces, however with some errors. For the spin up instance, the longitudinal force was estimated with a mean error of 6.10% and a maximum error of 21.9%, while the tire normal force was estimated with a mean error of 7.62% and a maximum error of 42.2%, see table 6.3. The better accuracy of longitudinal force estimation was traced to large fluctuations of the normal forces in the database at some of the relevant data points.

At the peak normal force instance the estimation has good accuracy except for a few data points. The accuracy of longitudinal force estimation at the peak normal force is lower, similar to what is noted at the spin up instance indicating that reliable and dense enough solutions are important for good accuracy of the algorithm. The mean error of the normal force is 1.04% while the longitudinal mean error is 25.9%, with the largest error being 214%, see table 6.4. The largest errors in longitudinal force were traced to missing data points in the database.

The accuracy of the spring back instance is the poorest, where the mean error of the normal force was 14.9% and the mean error for the longitudinal force was 26.2% with a noticeably largest error at 387%. For higher normal forces, an underestimating trend was noted, as well as for higher negative longitudinal forces. Further, all estimated forces were not that accurate, again indicating the importance of a good database. Further discussion of this can be found in section 6.2.4.

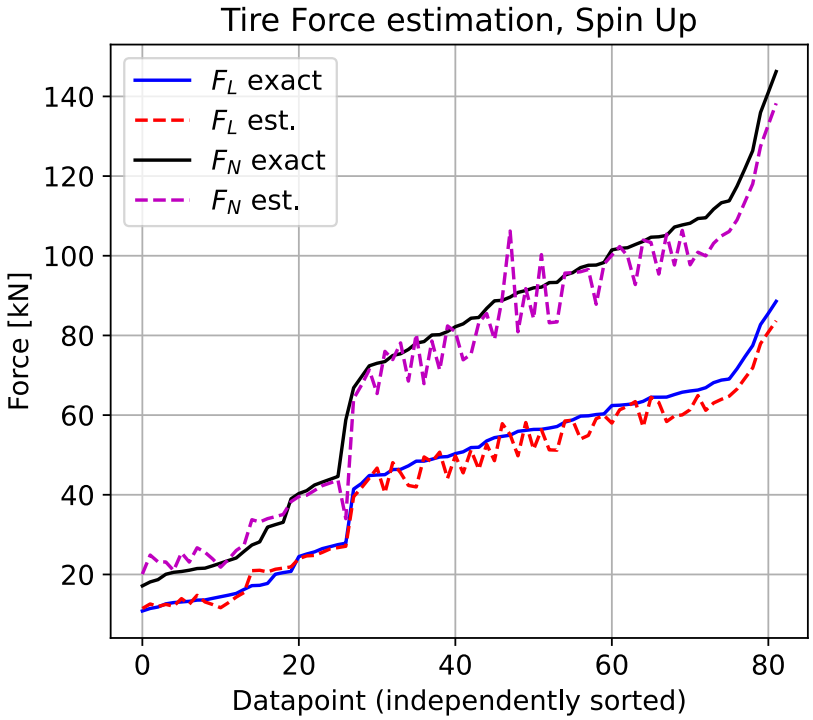

Figure 6.5: Validation runs results comparison, spin up instance. F_L is the longitudinal force and F_N the normal force.

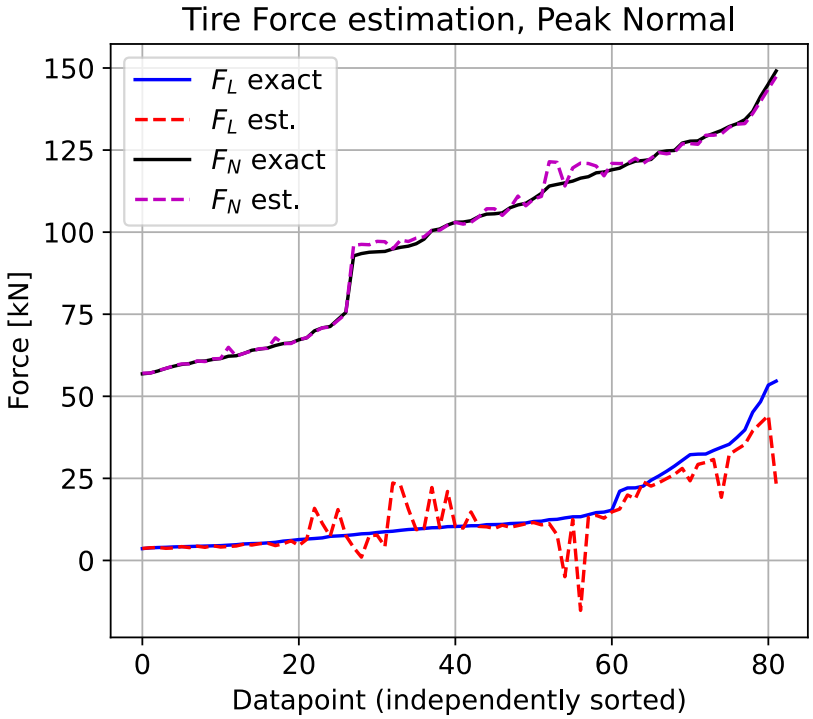

Figure 6.6: Validation runs results comparison, maximum normal force instance. F_L is the longitudinal force and F_N the normal force.

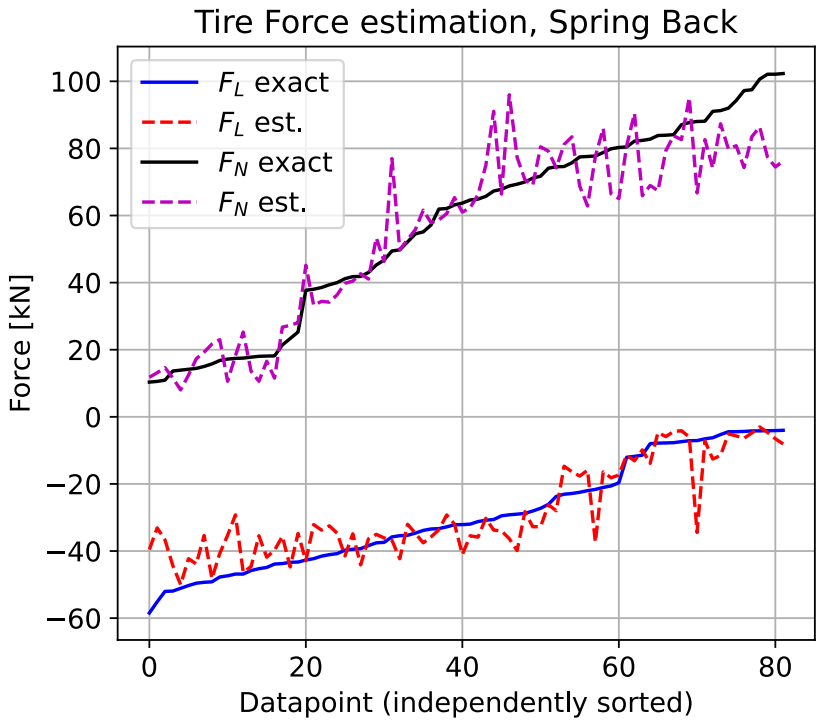

Figure 6.7: Validation runs results comparison, spring back instance. F_L is the longitudinal force and F_N the normal force

Table 6.4: Errors for different forces at peak normal force instance

	Mean error	Largest error	Smallest
Tire Normal	1.04%	6.49%	0.01%
Tire Longitudinal	25.9%	214%	0.05%
Tire Magnitude	1.15%	5.59%	0.00%

Table 6.5: Errors for different forces at spring back instance

	Mean error	Largest error	Smallest
Tire Normal	14.9%	55.8%	0.08%
Tire Longitudinal	26.2%	387%	0.22%
Tire Magnitude	15.5%	58.6%	0.25%

Table 6.6: Errors for different forces at the spin up instance with $\mu = 0.6$

	Mean error	Largest error	Smallest
Tire Normal	16.5%	66.7%	0.77%
Tire Longitudinal	430%	759%	33.8%
Tire Magnitude	24.9%	84.2%	1.10%

Table 6.7: Errors for different forces at the peak normal instance with $\mu = 0.6$

	Mean error	Largest error	Smallest
Tire Normal	3.96%	11.8%	0.06%
Tire Longitudinal	923%	22052%	5.36%
Tire Magnitude	4.91%	11.8%	0.25%

6.2.2 Effect of runway to tire friction

The algorithm was tested with respect to unknown runway friction and particularly estimating the forces at lower friction. A validation set was simulated with $\mu = 0.6$ instead of the regulatory $\mu = 0.8$. The reason was to understand whether it is of interest to consider the true friction rather than the high $\mu = 0.8$, which is the maximum friction that the gear will have to withstand during testing [7].

6.2.2.1 Result differences of reduced runway friction

Figures 6.8, 6.9 and 6.10 illustrate the estimated and exact normal and longitudinal forces. The longitudinal force is significantly overestimated since the database consists of force results where the friction is $\mu = 0.8$. Further, the error of the longitudinal force for all instances, see tables 6.6, 6.7 and 6.8, is extreme. This shows that the longitudinal force is highly dependent on friction and moreover that the friction will have to be known and included in the database and algorithm in order to obtain proper results. Alternatively, another method will have to be used.

The tire normal forces are also overestimated but at the peak normal instance only by a mean of 3.96%, see tables 6.6, 6.7 and 6.8. This shows that the tire normal force at peak normal instance has a small dependency of friction, some for spin up but large for spring back. One explanation for the large errors is not only the effect of lower friction itself but also that spin up and spring back occur at different time instances when the friction is changed. That means that the database peaks and lower friction peaks are not at the same time instances. The conclusion is that the tire normal force at peak normal instance can be estimated, while the estimation at the other instances is poor. Similarly to the longitudinal forces, the friction will have to be known to estimate these forces properly, or alternative methods will have to be used to improve the algorithm.

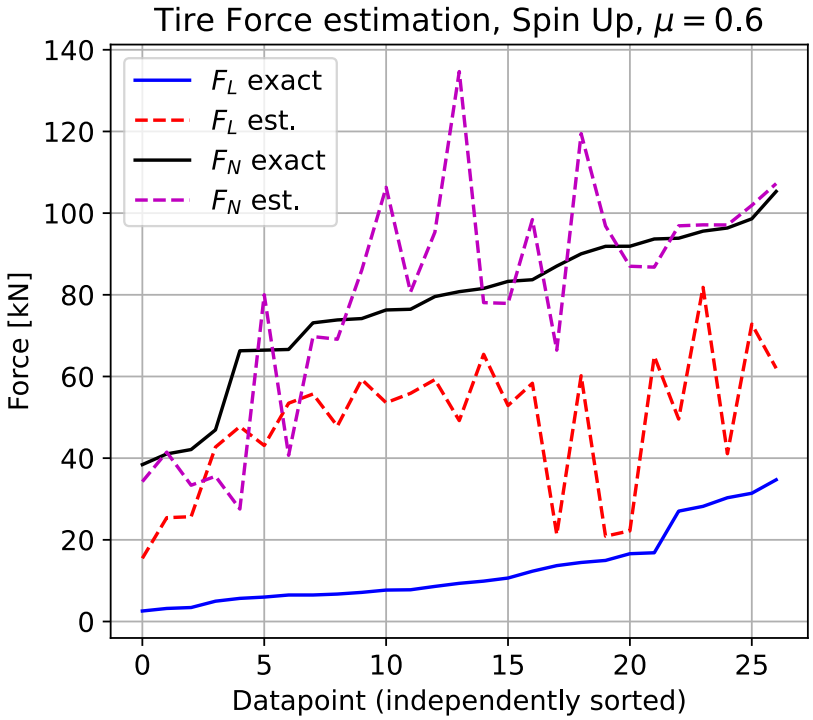

Figure 6.8: Low friction estimation, spin up instance. F_L is the longitudinal force and F_N the normal force.

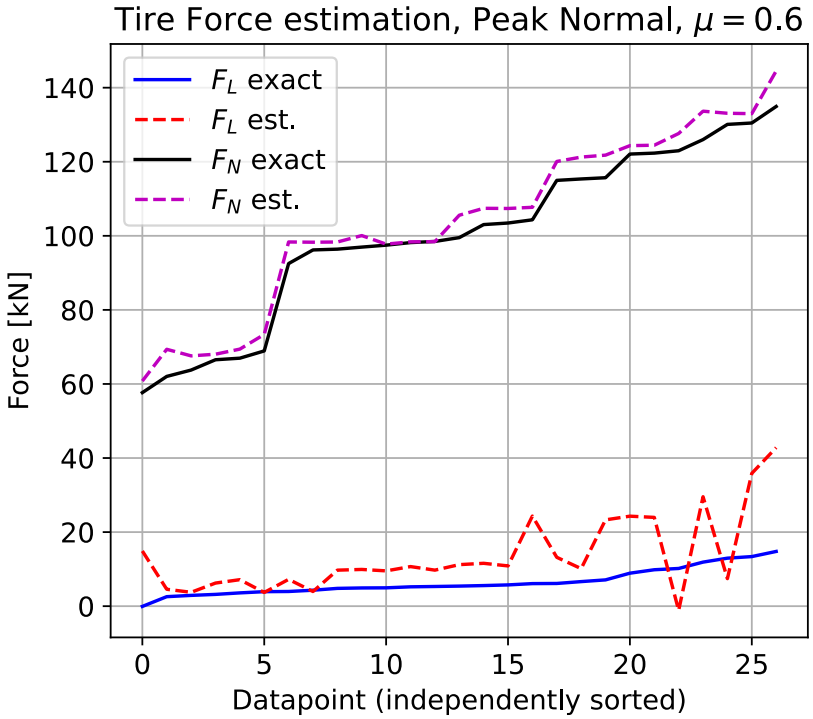

Figure 6.9: Low friction estimation, peak normal instance. F_L is the longitudinal force and F_N the normal force.

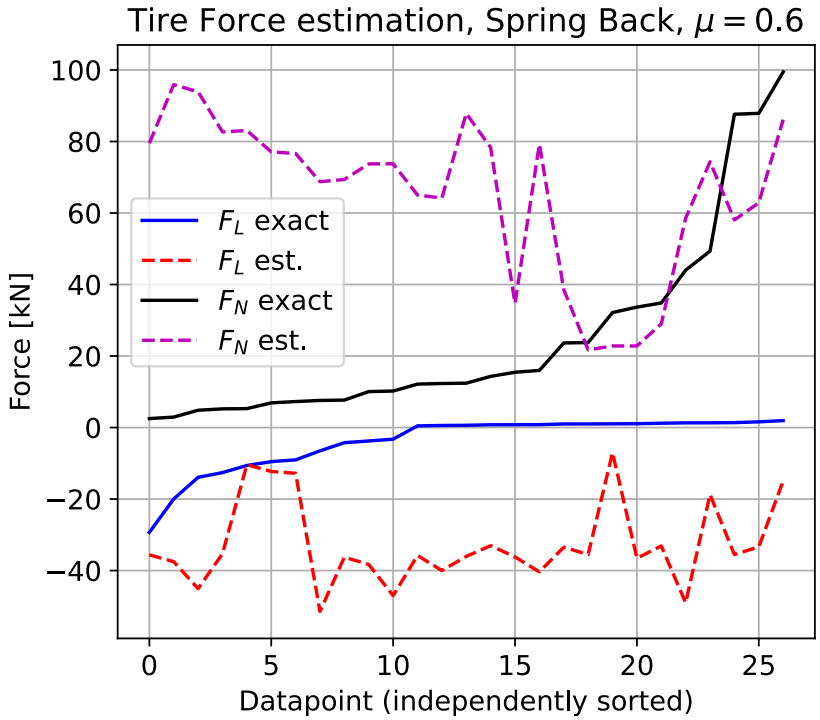

Figure 6.10: Low friction estimation, spring back instance. F_L is the longitudinal force and F_N the normal force.

Table 6.8: Errors for different forces at the spring back instance with $\mu = 0.6$

	Mean error	Largest error	Smallest
Tire Normal	690%	3180%	8.62%
Tire Longitudinal	2386%	7706%	2.15%
Tire Magnitude	754%	3356%	0.64%

Table 6.9: Errors for forces at the spin up instance with $p_{ao} = 18.5$ bar

	Mean error	Largest error	Smallest
Tire Normal	9.40%	39.9%	0.79%
Tire Longitudinal	7.59%	35.7%	0.66%
Tire Magnitude	8.90%	36.4%	0.76%

6.2.3 Effect of shock absorber servicing state

To test the effect of not knowing the shock absorber servicing state, a different spring curve was calculated using a lower initial gas pressure. The lower pressure $p_{ao} = 18.5$ bar compared to the proper at $p_{a0} = 22.5$ bar, which the shock absorber was designed for, was simulated with a validation set. Since the shock absorber model does not have a metering pin, it is not possible to test different damping characteristics. If the fluid is assumed to have leaked, however, the shock absorber would bottom out earlier. This is effectively shortening the stroke since the static displacement is greater than if the correct fluid amount is assumed. Since a bottoming would be critical for the S/A in itself, this is not investigated further.

6.2.3.1 Result differences of shock absorber servicing state

The tire forces at the peak normal instance can be seen in figure 6.11 while the tire forces at the spin up and spring back can be seen in appendix A.4 and A.5 respectively. The peak normal force can still be estimated by the algorithm with similar results as with $p_{ao} = 22.5$ bar, recall figure 6.6. This means that the peak tire forces are not significantly affected by changing the gas pressure in the shock absorber, at least for the lower initial pressure analyzed. This does not necessarily mean that other parts of the landing gear do not experience a different force, especially considering throughout the landing occurrence.

The error of the force estimations, presented in tables 6.9, 6.10 and 6.11, show that the spin up instance has an increased mean error and largest error for all estimated forces. At the peak normal instance, the tire normal force and tire magnitude errors are acceptable, however longitudinal error is increased, particularly the largest error. In the spring back instance the error trends are similar to peak normal but magnified. Evidently, the longitudinal forces are estimated with less accuracy, especially the largest error for the spring back instance, which is at 679%.

While the errors for longitudinal force estimation are not sufficient, the tire magnitude error is similar to the tire normal, indicating that the longitudinal forces are small compared to the normal. Thus, the tire normal forces are critical for overload detection, and since these can be estimated with similar errors as with the intended initial pressure there is no need for alternative methods. This does, however, not conclude anything about the effect of damping.

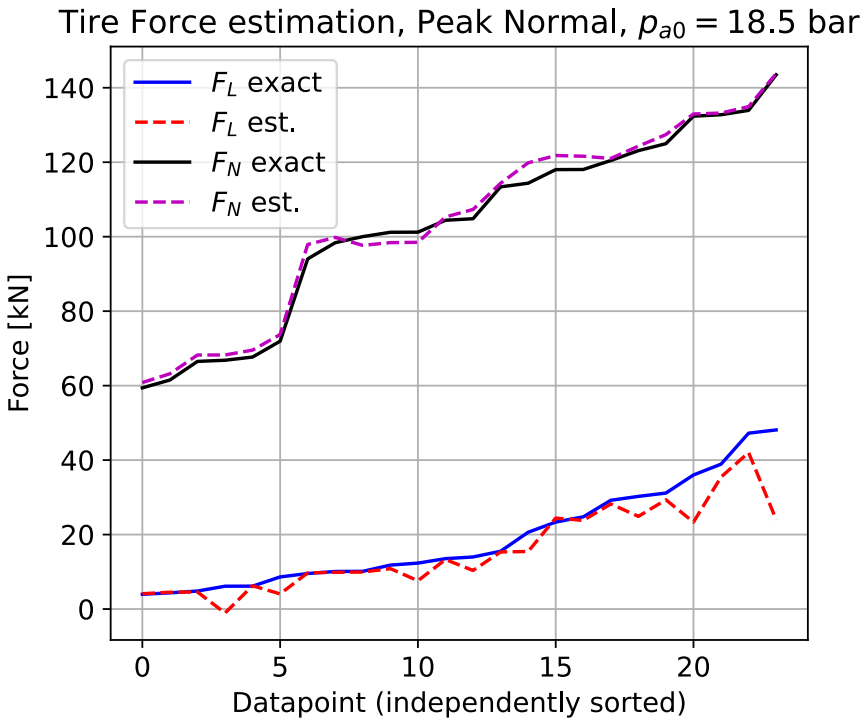

Figure 6.11: Low gas pressure estimation at peak normal instance. F_L is the longitudinal force and F_N the normal force.

Table 6.10: Errors for forces at the peak normal instance with $p_{ao} = 18.5$ bar

	Mean error	Largest error	Smallest
Tire Normal	2.03%	4.79%	0.24%
Tire Longitudinal	18.0%	117%	1.22%
Tire Magnitude	1.97%	5.84%	0.07%

Table 6.11: Errors for forces at the spring back instance with $p_{ao} = 18.5$ bar

	Mean error	Largest error	Smallest
Tire Normal	15.3%	61.1%	0.38%
Tire Longitudinal	50.4%	679%	1.63%
Tire Magnitude	15.2%	61.8%	1.91%

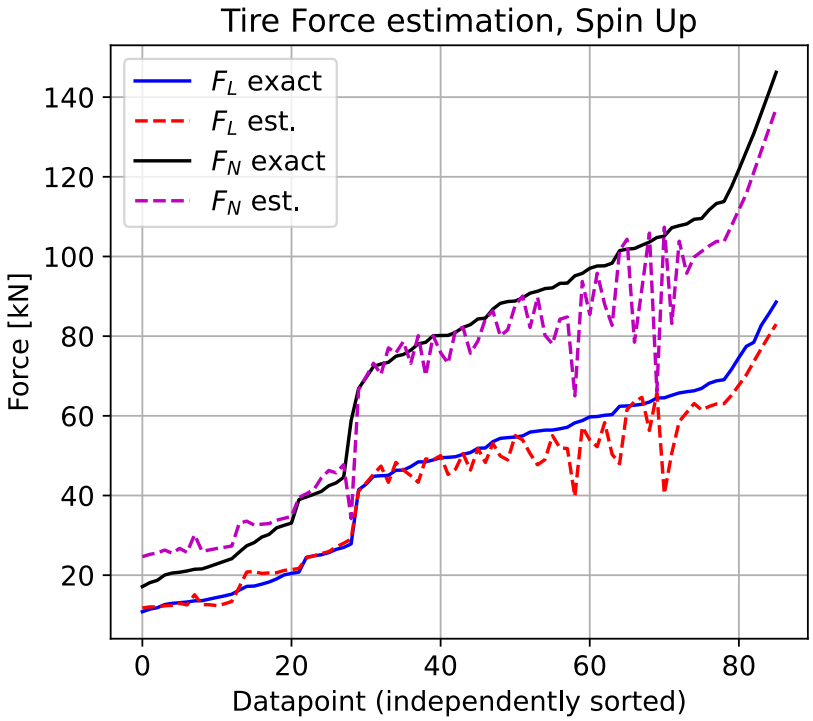

Figure 6.12: peak normal instance with reduced database. F_L is the longitudinal force and F_N, the normal force.

6.2.4 Databse density

In order to investigate if the data points in the database were dense enough to not induce errors, the algorithm was edited to exclude every other data point in regards of vertical velocity, effectively half the database. While the reduction of the database is significant for this test, it was performed to understand if a reduced database can provide similar results, or if the errors are drastically increased.

A plot of the estimation at the spin up instance with a reduced database can be seen in figure 6.12, with errors presented in table 6.12. When comparing with the full database in figure 6.5 and errors in table 6.3, larger errors are recorded but not a drastic change. This provides information that a dense database can estimate forces with better accuracy.

Linear interpolation was used and is a key factor in the increase in error when reducing the database density due to the non-linear Pareto surfaces. To reduce the error other types of interpolation methods could be investigated, for example Shephard's method [21].

Table 6.12: Errors for different forces at spin up instance with a reduced database

	Mean error	Largest error	Smallest
Tire Normal	11.1%	43.8%	0.00%
Tire Longitudinal	7.46%	37.3%	0.06%
Tire Magnitude	9.71%	37.0%	0.02%

6.3 Alternative method for tire longitudinal force

As noticed when testing a different friction coefficient, the longitudinal force is, as expected, highly sensitive to the friction coefficient. One way of improving this estimation is to use the wheel's angular momentum to predict the longitudinal force in the contact patch. Since most aircrafts are equipped with a wheel speed sensor, this can be considered an already existing input just as the flight data used. This method has been investigated for drop tests already, see Wang, Wu and Wang [22].

6.3.1 Theory behind wheel speed sensor as force prediction

The angular momentum of the wheel assembly can be described as

$$L = I\omega(t) \tag{6.1}$$

with L being the angular momentum, I the moment of inertia and ω the angular velocity of the wheel [20, p.9]. Further, the law of angular momentum [20, p.9] gives

$$\sum M = \dot{L}. \tag{6.2}$$

The torque of the wheel assembly at the wheel center from the tire longitudinal force can be described as

$$M = F_x R(t) \tag{6.3}$$

where F_x is the longitudinal force on the tire contact patch and R is the tire radius. Combining equation (6.1), (6.2) and (6.3) gives the equation which describes the longitudinal tire force as a function of angular velocity:

$$F_x(t) = I(\dot{\omega}(t) - \dot{\omega}_0)/R(t). \tag{6.4}$$

6.3.2 Force estimation using wheel speed sensor

The use of equation 6.4 instead of the database was implemented in the algorithm to calculate the longitudinal force, while the normal force was still estimated from the database as before. Note that for this implementation, the assumptions of a time constant moment of inertia and tire radius were made, simplifying the calculation.

6.3.2.1 Result of using wheel speed sensor for longitudinal force estimation

As can be seen in figure 6.13, 6.14 & 6.15 for the three critical instances during landing, the longitudinal force can accurately be estimated with the wheel speed

Table 6.13: Errors for tire forces at the spin up instance with $\mu = 0.8$ when using the angular momentum to estimate the longitudinal force

	Mean error	Largest error	Smallest
Tire Normal	7.44%	24.3%	0.30%
Tire Longitudinal	14.3%	25.1%	4.63%
Tire Magnitude	7.28%	22.8%	0.22%

sensor for the validation runs with $\mu = 0.6$. While the estimation is better, the force is underestimated for all data points. This is a result of the assumed constant undeformed tire radius. The tire radius is in reality decreasing with higher loads during the landing event. The inertia properties are also changing due to the unsymmetrical deformation of the tire, however not with the same impact as the leverage arm of the tire radius itself.

This underestimation can also be seen when the regulatory friction is used, illustrated in figure 6.16. The mean error of the longitudinal force when $\mu = 0.8$ in the spin up case is 14.3% which can be compared to the mean error of 6.10% when using the database to estimate the force. This shows that higher accuracy can be achieved using the database to estimate the longitudinal force if the friction is known for the landing and in the database. Correct measure of the friction is however cumbersome to obtain for each landing case.

Even though the estimation of longitudinal force based on the wheel acceleration has worse accuracy than using the database for known friction, the error when the friction is unknown is significantly decreased. This can be seen by comparing tables 6.14, 6.15 & 6.16 with tables 6.6, 6.7 & 6.8. There is an exception of one data point in the spring back instance in figure 6.15. Thus, there is potential to use an angular velocity sensor to estimate the longitudinal force, if the tire radius is known or the deflection is small. One example to increase the accuracy of the method is to approximate the radius from the vertical tire force and the tire vertical stiffness.

Aspects of special consideration opposing the alternative method of using wheel speed sensors for estimating the longitudinal force is slip or skid of the wheel. In a case where high slip occurs, the wheel speed would not represent the force without additional terms in the expression which would be cumbersome to implement and measure. Further, in a full skid scenario, say for example if a wheel has locked up, the lateral force estimated would be zero, obviously not correctly estimated.

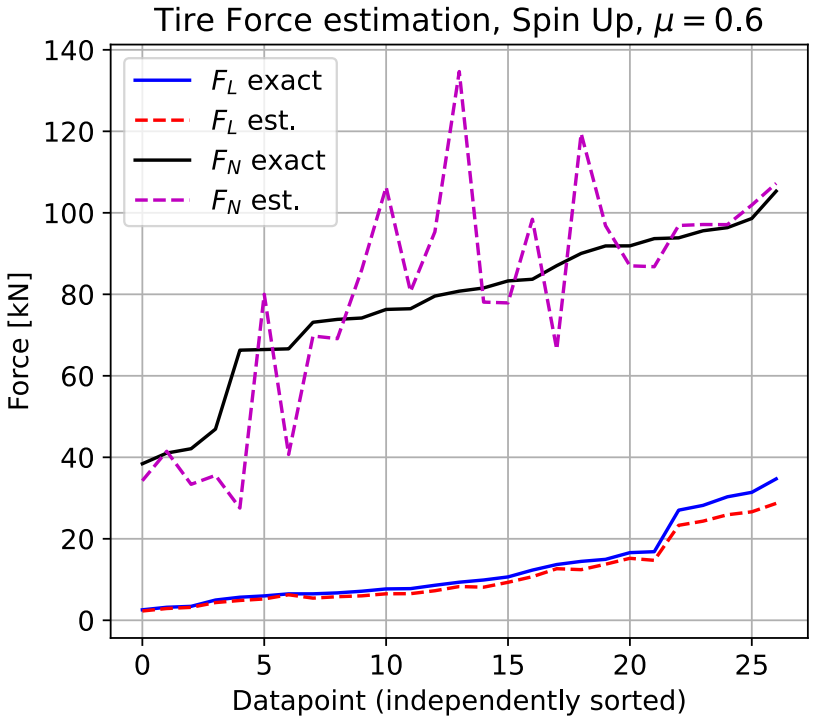

Figure 6.13: Wheel speed estimation at spin up, low friction. F_L is the longitudinal force and F_N the normal force.

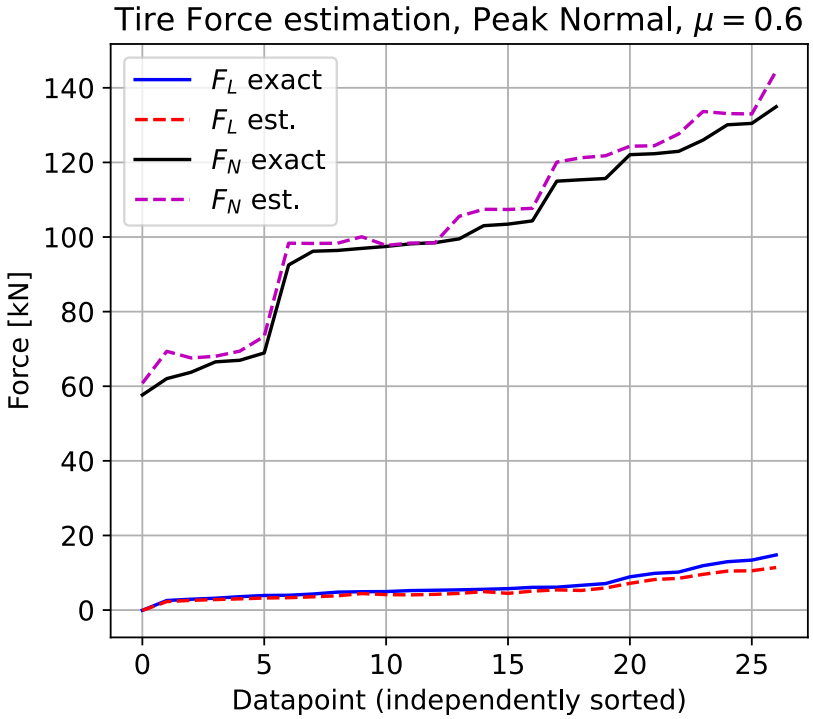

Figure 6.14: Wheel speed estimation at peak normal, low friction. F_L is the longitudinal force and F_N the normal force.

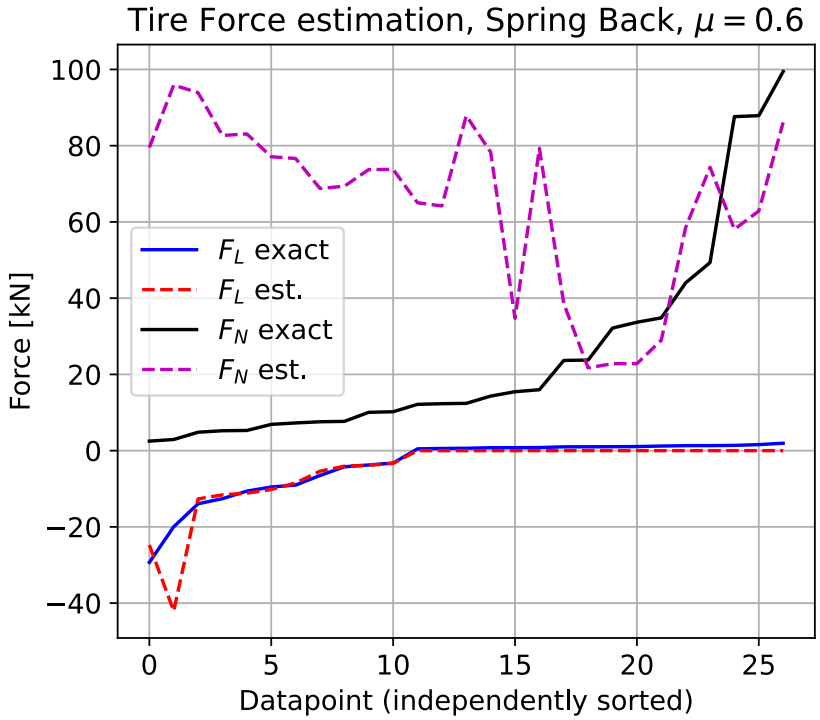

Figure 6.15: Wheel speed estimation at spring back, low friction. F_L is the longitudinal force and F_N the normal force.

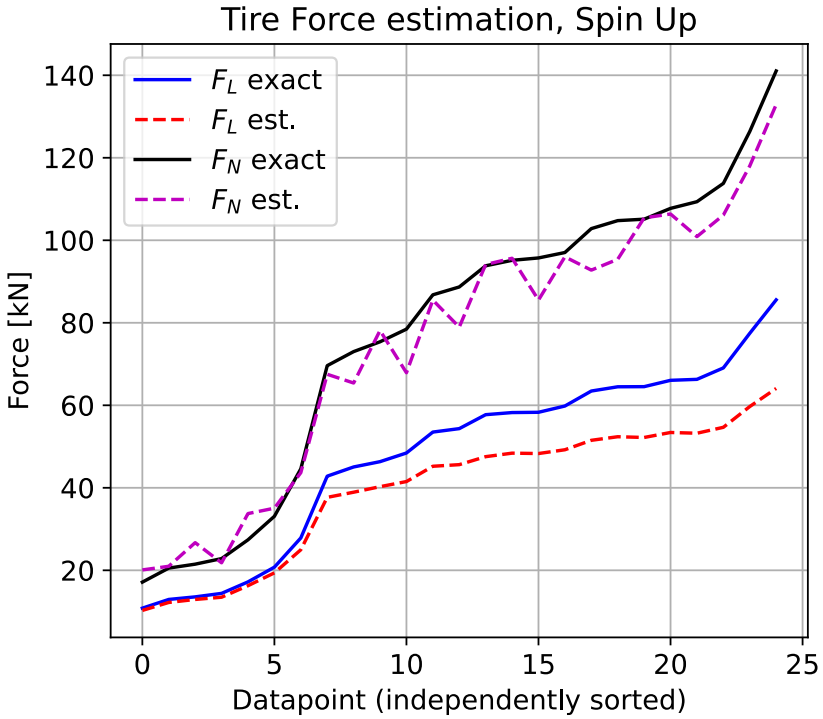

Figure 6.16: Wheel speed estimation at spin up, regulated friction. F_L is the longitudinal force and F_N the normal force.

Table 6.14: Errors for tire forces at the spin up instance with $\mu = 0.6$ when using the angular momentum to estimate the longitudinal force

	Mean error	Largest error	Smallest
Tire Normal	16.5%	66.7%	0.77%
Tire Longitudinal	12.7%	17.8%	3.51%
Tire Magnitude	24.9%	84.2%	1.10%

Table 6.15: Errors for tire forces at the peak normal force instance with $\mu = 0.6$ when using the angular momentum to estimate the longitudinal force

	Mean error	Largest error	Smallest
Tire Normal	3.96%	11.8%	0.06%
Tire Longitudinal	18.1%	44.4%	10.0%
Tire Magnitude	4.91%	11.8%	0.25%

Table 6.16: Errors for tire forces at the spring back instance with $\mu = 0.6$ when using the angular momentum to estimate the longitudinal force

	Mean error	Largest error	Smallest
Tire Normal	690%	3180%	8.62%
Tire Longitudinal	66.2%	110%	1.96%
Tire Magnitude	754%	3357%	0.64%

7
Discussion

From the results and discussions conveyed throughout the report, several aspects of importance are covered below.

7.1 Lift force assumption

The assumption that the lift to weight ratio is 1, made in Section 5.1.2 is valid during drop test but not necessarily during an aircraft landing, where the lift may vary over time. Since the lift to weight ratio of 1 was used, the results are not conservative since a lower lift would result in higher loads. A better estimation of the force could be obtained by modeling the lift force instead and including it as an input to the algorithm. This is also a requirement for a full aircraft model, as the equivalent weight formulation is only valid for drop tests.

7.2 Stress in parts, dependent on S/A stroke

At the three instances during a landing, spin up, spring back and peak normal force, the load has been estimated. To further extend the understanding, the next step would be to estimate the stress at these instances. To make a good estimation of the stress, the stroke will have to be known since the landing gear leg position has a significant impact on the load application. This in turn affects the straining of the individual landing gear parts. The stroke could potentially be estimated in the same manner as the algorithm is estimating the tire forces currently. This would mean to include the shock absorber stroke as a batch run simulation result in the database.

7.3 Non-linear interpolation

It would be interesting to investigate whether a non-linear interpolation technique or graph regression method, using several points in the database, could estimate the tire forces more accurately. Since some simulations failed and the fact that the database has non-linear solution Pareto surfaces, a non-linear estimation would be expected to be more accurate. With a non-linear interpolation, the database could potentially consist of less points, which means less simulation time and less data to store. This would be of great importance if more parameters would be included

as inputs. While a non-linear algorithm might need less data stored, the actual estimation could take longer time.

7.4 Ground and taxi loads

With the algorithm created no ground or taxi loads can be estimated even though these can be critical during not only landing but also towing or take off. This is because the shock absorber is already compressed and the aircraft may be at MTOM. The loads could perhaps be estimated by using a different method, for example if accelerometers placed on the landing gear are used instead.

7.5 Fatigue estimation

No fatigue estimations have been conducted in the thesis but there is a potential for fatigue estimation by saving the forces at the three instances and considering the stresses in the parts of the landing gear. From the stress peaks, a load cycle could be established and fatigue could be estimated over time. This fatigue estimation would however only conclude the force peaks at these instances and would not include any taxing or towing loads. With the algorithm created though, the forces could indicate if the loads applied to the landing gear in general is higher or lower than what the gear has been designed for, effectively indicating if the design assumptions are conservative to give input to future landing gear designs.

7.6 Shock absorber force

In the algorithm, estimating the tire forces has been the focus since the load path through the entire landing gear can be derived from these forces. Even though the S/A force can be derived from the tire forces, an attempt to use the algorithm to estimate it was done and showed promising results even though the S/A force estimation gave large errors for high loads. The large errors were traced to the S/A being close to bottoming out in many upper data points in the database, for which the maximum loads were extreme. In a more dense database, the estimation would be performed with respect to forces from data points where the S/A has not bottomed out, from which more promising results are expected.

8
Conclusions

From the work that has been conducted in the thesis some conclusions can be drawn about using flight parameter data for hard landing detection.

8.1 The algorithm

An algorithm has been created which estimates the force from a database. The data has been created with multi-body dynamic simulations and interpolating between data points based on input parameters. It was shown that the algorithm can estimate the force somewhat accurate but that the tire forces were sensitive to friction, especially the longitudinal force.

The algorithm was also tested for an assumed S/A leak, effecting the stiffness but not the damping. The algorithm showed similar results to the case without leakage. An even lower initial pressure could be tested to ensure that the estimation is valid for extreme cases. But primarily to model a varying damping would be of interest, which would require a different S/A model.

An alternative way to estimate the longitudinal force was also introduced because of the friction sensitivity. This alternative used the angular velocity of the tire to estimate the longitudinal force independent of the friction between the tire and runway. It resulted in a more accurate method if the tire deformation is small and friction is unknown, assuming that no slip or skid occurs.

In general, the tire normal force for different frictions can be estimated at the peak normal case with the algorithm, while the estimation is deficient at the spin up and spring back case. Using the angular velocity of the tire gave a better estimation of the longitudinal force, while always underestimating it due to assuming an undeformed tire radius.

8.2 Future work

The thesis was aimed at creating an algorithm for detecting hard landings. A part of that was done but more work is needed in order to get a complete algorithm. Other parts that would have to be implemented for the detection to work in commercial use are to translate the data gathered in the flight data recorder (FDR), not necessarily located at the drop mass as in the drop test model used, to initial

conditions for the algorithm.

As discussed, a denser database would be needed for reliable use in commercial aircraft. As an extent, the linear interpolation should be changed to a more accurate interpolation method to reduce the error seen in the results. The tire deformation would need to be included in the database or estimated in some manner to improve the alternative method using wheel speed sensors for tire longitudinal force estimation, for example by considering the tire vertical stiffness and tire normal force. This is also true for the change in inertia which is expected to have an impact on the alternative longitudinal force estimation, while not as significant as the tire radius change.

Further, all landing gears should be modeled under real landing events instead of a single landing gear under drop test scenario. This would not only extend to include landings with aircraft roll, but also yaw, introducing lateral forces which would need consideration. Not only this, but effects of accelerations in all directions will have an impact on the loads, which would also need to be included as input parameters.

Another step would be to create an algorithm to decide if a combination of forces actually is a hard landing, especially for combinations of forces resulting in force vectors with different directions, relating to different stresses in the landing gear components. This would entail structural simulations for a large amount of load combinations to provide proper thresholds. Further, the stress in the landing gear will be dependent on the stroke of the shock absorber, which means that the stroke at the three instances would need to be known. This is a significant amount of work as there are multiple failure modes that would need to be considered for example, shear failure, bending, tension and compression.

A flow chart of an extended algorithm needed in order to implement the concept on an aircraft is shown in figure 8.1, where the dashed line indicates the parts implemented in this thesis. The box "Estimate forces" includes the flow chart presented in figure 6.4. The pitch, θ, vertical velocity, V_z, longitudinal velocity V_x and the mass, m that the landing gear is subjected to, are initial conditions for the interpolation algorithm. The angular velocity of the wheel, ω, is the input to the alternative method to estimate the longitudinal force.

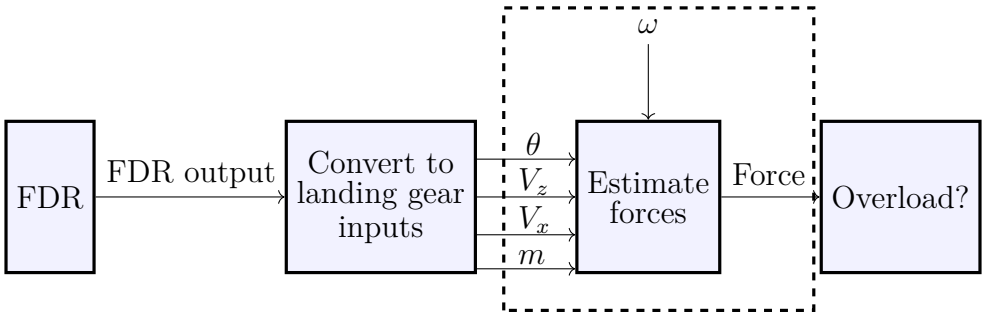

Figure 8.1: Flow chart of an extended algorithm needed for the concept to work on an aircraft. The dashed outline indicates the parts implemented in this thesis.

Bibliography

[1] SAE International, "AIR 6813 - Landing gear manufacturing, maintenance, repair, and overhaul critical process", Issued: 09.05.2022, Accessed: 17.01.2023, Available: www.sae.org/standards/content/air6813

[2] Infosys, "Aircraft Landing Gear Design & Development", Published 2018

[3] SAE International, "AIR5938A - Information on Hard Landings and Abnormal Landing Gear Loading Events", Revised: 20.12.2019, Available: www.sae.org/standards/content/air5938a

[4] SAE International, "AIR6168A - Information on Hard Landings and Abnormal Landing Gear Loading Events", Revised: 23.05.2019, Accessed: 18.01.2023, Available: www.sae.org/standards/content/air6168a

[5] Bradley, W. Baird, "Overload Detection/Health Monitoring Landing Gear Sensor System Proposal", Published: 2008.

[6] cascade, "How to create a decision matrix", Published: 24.10.2022, Accessed: 30.05.2023, Available: https://www.cascade.app/blog/how-to-create-a-decision-matrix

[7] EASA, "Certification Specifications and Acceptable Means of Compliance for Large Aeroplanes (CS-25) - Amendment 27", Published 24.11.2021, Available: www.easa.europa.eu/en/document-library/certification-specifications/cs-25-amendment-27

[8] Robert Kyle Smith, "The Design of Aircraft Landing Gear Vols. I & II", Published: 18.02.2021, SAE International

[9] Dassault Systemes, "Shape the world we live in", Available: https://www.3ds.com/products-services/catia/

[10] Norman Currey, "Aircraft Landing Gear Design - Principles and Practice", Published: 1988

[11] MSC Adams, "Adams 2021.2 - Online Help", Available: help.hexagonmi.com/bundle/adams_2021.2/page/adams_main.htm

[12] NASA, Robert F. Smiley and Walter B. Horne, "Mechanical Properties Of Pneumatic Tires With Special Reference To Modern Aircraft Tires", Published: January 1958, Available: ntrs.nasa.gov/api/citations/19930084870/downloads/19930084870.pdf

[13] Michelin, "Aircraft Tire Engineering Data", Accessed: 03.03.23, Available: https://www.jupitor.co.jp/pdf/michelin_aircraft.pdf

[14] Goodyear Aviation Tires, "Goodyear Aviation Tire, Three-Part Tire Specifications", Accessed: 03.03.23, Available: www.goodyearaviation.com/resources/pdf/Data-Section-2022.pdf

[15] Dunlop Aircraft Tires, "General Practices Manual for Aircraft Tyres and Tubes", Published: September 2021, Available: www.dunlopaircrafttyres.co.uk/media/1258/dm1172_september_2021.pdf
[16] SAE International, "ARP5644 - Landing Gear Shock Absorption Testing of Civil Aircraft", Revised: 14.07.2020, Available: www.sae.org/standards/content/arp5644
[17] Skybrary, "Approach Speed Categorisation", Accessed: 10.03.2023, Available: www.skybrary.aero/articles/approach-speed-categorisation
[18] Boeing, "Tail Strikes: Prevention", Available: www.boeing.com/commercial/aeromagazine/articles/qtr_1_07/AERO_Q107_article2.pdf
[19] Infinidim, "Boeing 777 Tail Clearances", Available: www.infinidim.org/wp-content/uploads/2015/01/Rotation6.jpg
[20] M.M. Japp, "*Formulas in mechanics*", Gothenburg, Sweden: Chalmers, 2010.
[21] Wikipedia, "Inverse distance weighting", Accessed: 29.05.2023, Available: https://en.wikipedia.org/wiki/Inverse_distance_weighting
[22] Wang, Wu & Wang, "A New Method for Determining Horizontal Impact Load Based on Rotational Speed of Aircraft Wheel in Landing Gear Drop Test", Published: 10.07.2017, Available: www.matec-conferences.org/articles/matecconf/abs/2017/28/matecconf_2mae2017_03004/matecconf_2mae2017_03004.html

A

Appendix

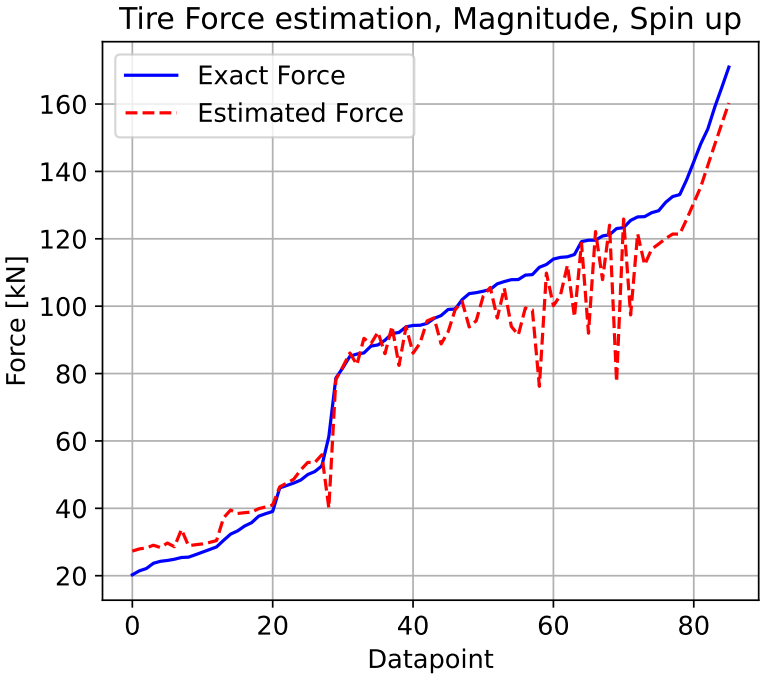

Figure A.1: Validation runs results comparison, force magnitude, spin up instance

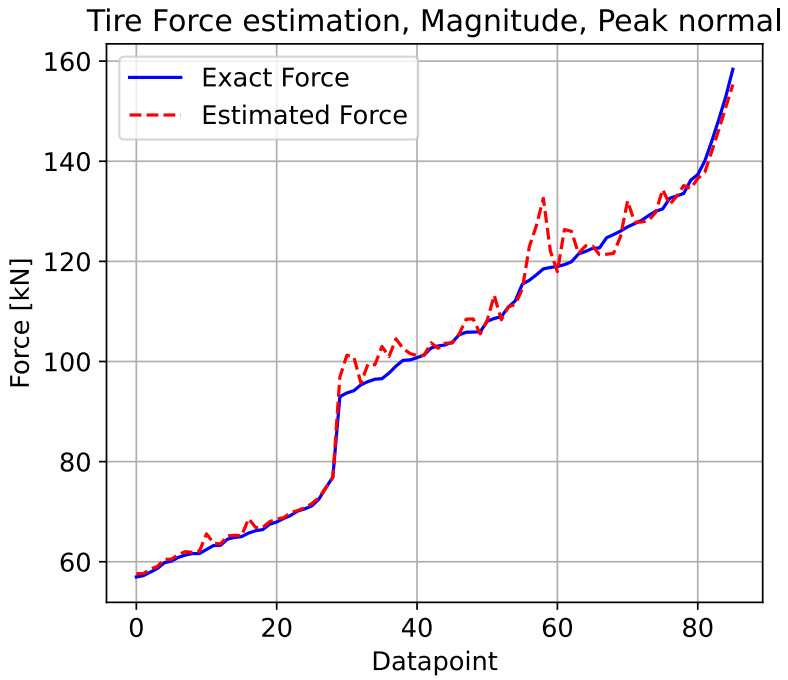

Figure A.2: Validation runs results comparison, force magnitude, peak normal instance

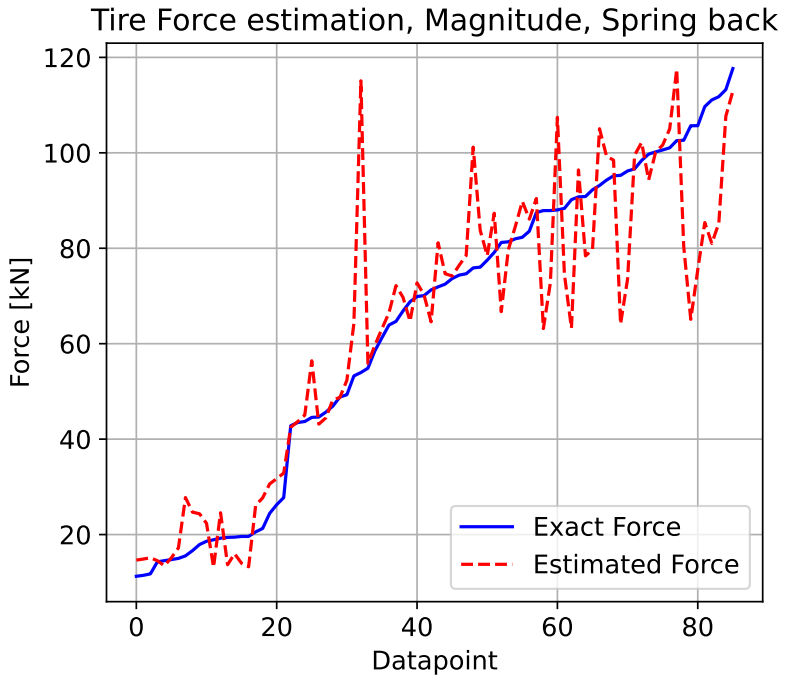

Figure A.3: Validation runs results comparison, force magnitude, spring back instance

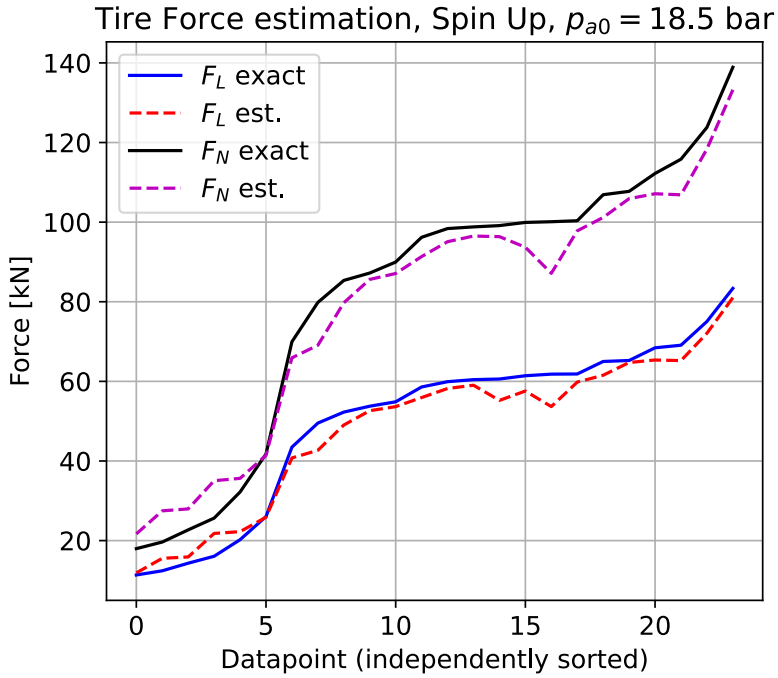

Figure A.4: Low gas pressure force estimation, spin up instance

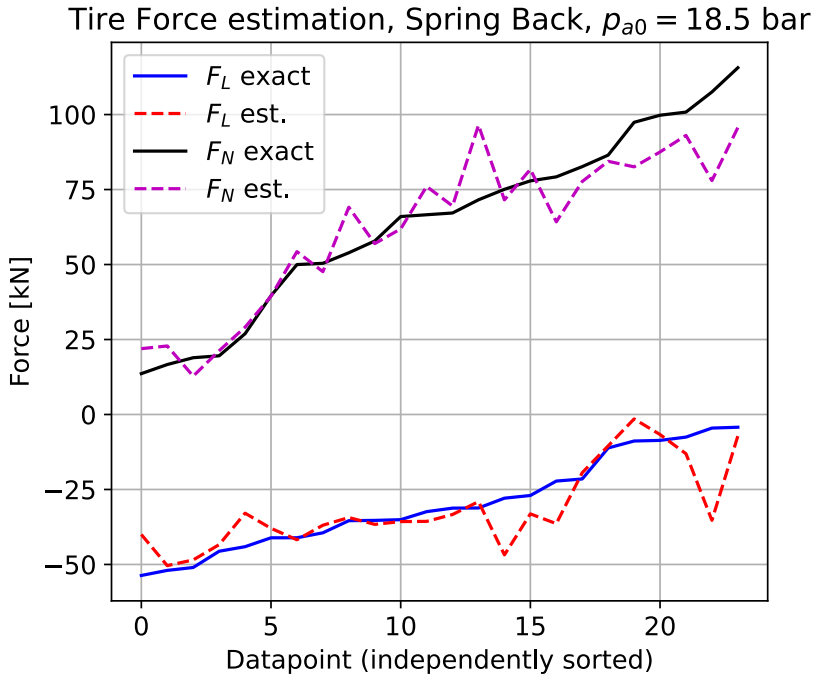

Figure A.5: Low gas pressure force estimation, spring back instance

DEPARTMENT OF INDUSTRIAL AND MATERIALS SCIENCE
CHALMERS UNIVERSITY OF TECHNOLOGY
Gothenburg, Sweden
www.chalmers.se

CHALMERS
UNIVERSITY OF TECHNOLOGY